Supporting Information

A highly stable, planar thiophene-fused triarylborane as a new building block for semiconductor polymers

Yohei Adachi,*[1] Ryuji Matsuura,[1] Hiroki Tobita,[1] Tsubasa Mikie,[2] Itaru Osaka[2] and Joji Ohshita*[1,3]

[1] *Smart Innovation Program, Graduate School of Advanced Science and Engineering, Hiroshima University, Higashi-Hiroshima 739-8527, Japan. E-mail: yadachi@hiroshima-u.ac.jp, jo@hiroshima-u.ac.jp*

[2] *Applied Chemistry Program, Graduate School of Advanced Science and Engineering, Hiroshima University, Higashi-Hiroshima 739-8527, Japan.*

[3] *Division of Materials Model-Based Research, Digital Monozukuri (Manufacturing) Education and Research Center, Hiroshima University, Higashi-Hiroshima, Hiroshima 739-0046, Japan.*

Email: yadachi@hiroshima-u.ac.jp (YA), jo@hiroshima-u.ac.jp (JO)

Experimental

Materials

All reactions were performed under an argon atmosphere. The reaction solvents (diethyl ether, THF, cyclopentyl methyl ether (CPME), and dichloromethane) were purchased from Kanto Chemical Co., Ltd., distilled from calcium hydride, and stored over activated molecular sieves under argon prior to use. All other chemicals were purchased from FUJIFILM Wako Pure Chemical Corporation or TCI Co., Ltd. The starting materials **NDI-Br**[S1] and **DPP-Br**[S2] were prepared according to literature procedures. NMR spectra were recorded on Varian System 500 and 400MR spectrometers. The abbreviations Th and Bz used in the NMR assignments denote thiophene and benzene ring, respectively. High-resolution APCI mass spectra were obtained on a Thermo Fisher Scientific LTQ Orbitrap XL spectrometer at the Natural Science Center for Basic Research and Development (N-BARD), Hiroshima University. Molecular weight determinations were performed by GPC using an HLC8321GPC/HT system equipped with columns (TSKgel GMHHR-H(S)HT2). *o*-DCB was used as the eluent at 140 °C with a flow rate of 1.0 mL/min, and the molecular weights were calibrated against polystyrene standards. Thermogravimetric analysis (TGA) was conducted on an SII TG/DTA-6200 analyzer under a nitrogen flow (30 mL/min) at a heating rate of 10 °C/min.

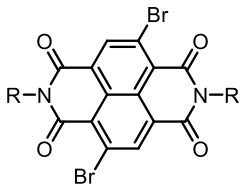

R = 2-octyldodecyl

NDI-Br

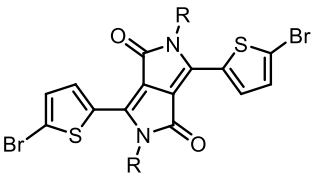

R = 2-dodecylhexadecyl

DPP-Br

XRD measurements

Single crystal X-ray diffraction data for **DTTB** were collected at 100 K on a Rigaku XtaLAB Synergy-R/DW diffractometer at N-BARD, Hiroshima University, using MoKα radiation monochromated with a multilayered confocal mirror. The structure was solved by intrinsic phasing using the HELXT-2018/2 program and refined using Fourier techniques. Non-hydrogen atoms were refined anisotropically, while hydrogen atoms were included in the model but not refined (SHELXL-2018/3). All other calculations were performed using the Olex2 software package. Graphical crystal structures were generated using Mercury 4.3.1 (Cambridge

Crystallographic Data Centre).

Optical measurements

UV–vis absorption spectra were measured with a Shimadzu UV-3600 Plus spectrometer. PL spectra, phosphorescence lifetimes, and absolute PL quantum yields were measured with a HORIBA FluoroMax-4 spectrophotometer equipped with an integrating sphere. Fluorescence lifetimes were measured on a HORIBA DeltaFlex modular fluorescence lifetime system, using a Nano LED pulsed diode as the excitation source. The sample concentrations were 10 μmol/L. A quartz cuvette with an optical path length of 1.0 cm was used for the measurements, and the background was corrected using the double-beam method. Molar absorption coefficients were calculated according to the Lambert-Beer law ($A = \varepsilon cl$, A: absorbance, ε: molar absorption coefficient, l: optical path length, c: concentration).

Electrochemical measurements

Cyclic voltammetry measurements were performed with an AMETEK VersaSTAT 4 potentiostat/galvanostat in an acetonitrile solution containing 0.1 M tetrabutylammonium hexafluorophosphate ($TBAPF_6$). A three-electrode system was employed, consisting of a Pt plate counter electrode, a Pt wire working electrode, and an Ag/Ag^+ reference electrode. The potentials were calibrated using ferrocene as an external standard. To prepare the working electrode, the polymer (1 mg) and $TBAPF_6$ (10 mg) were dissolved in 1 mL of chlorobenzene, and the resulting solution was drop-casted on the electrode and dried under vacuum at 50 °C for 2 h.

DFT calculations

The S_0 geometries were optimized via DFT calculations using the Gaussian 16 program at the B3LYP/6-31G(d) level of theory. TD-DFT calculations were performed at the same level. NICS calculations were carried out at the B3LYP/6-31G(d,p) level on the optimized S_0 geometries. Fluoride ion affinity (FIA) calculations were performed at the M06-2X(D3zero)/def2-QZVPP//B3LYP-D3(BJ)/6-31G(d) level. The FIA value was calculated using the experimental FIA value of Me_3Si^+ (952.5 kJ/mol) as a reference. The S_1–T_1 energy gap

(ΔE_{ST}^{DFT}) was determined as the difference between the first excitation energies obtained from TD-DFT calculations at the B3LYP/6-31G(d) level, using the respective geometries of S_0 and T_1 optimized at the same level of theory.

OFET device fabrication and characterization

Top-gate-bottom-contact (TGBC) devices were fabricated on an alkali-free glass substrates, on which Cr/Au source and drain electrodes were patterned via photolithography. The glass substrates were cleaned by ultrasonication in isopropanol for 10 min, followed by rinsing in boiled isopropanol for 10 min, and subsequent UV-ozone treatment for 30 min. The cleaned substrates were treated with 1-octanethiol to modify the Au source and drain electrodes. Thin films of **P1** and **P2** were spin-coated from chloroform solutions (5 mg mL^{-1}) and then annealed at 100 ℃ for 10 min. A CYTOP dielectric layer (C_i = 4.13 nF cm^{-2}) with a thickness of ca. 450 nm was spin-coated onto the active layer and subsequently dried at room temperature for 12 h. Finally, a 100 nm Ag layer was evaporated through a shadow mask as the gate electrode. Current-voltage characteristics were measured at room temperature under vacuum using a KEYSIGHT B2902A and a semiconductor parameter analysis software (SYSTEMHOUSE SUNRISE). Threshold voltages were estimated from the transfer plots by extrapolating the square root of the drain current to the horizontal axis. Field-effect mobilities were extracted from the square root of the drain current in the saturation regime according to the following equation:

$$\mu = \frac{2L}{WC_i}\left(\frac{d\sqrt{|I_d|}}{dV_g}\right)^2$$

where L (25 μm) and W (10,000 μm) are the channel length and width, respectively, and C_i is the capacitance of the gate insulator. Average hole and electron mobilities and threshold voltages were calculated from at least eight devices.

OPV fabrication and characterization

ITO-coated glass substrates were sequentially pre-cleaned by ultrasonication in a detergent bath, deionized water, acetone, and isopropanol at room temperature, followed by boiled isopropanol for 10 min each, and were finally baked at 120 ℃ for 10 min in air. The substrates were then subjected to UV/ozone treatment at

room temperature for 10 min. A ZnO electron-transporting layer was deposited by spin-coating (1200 rpm, 10 s) from a dilute dispersion of ZnO nanoparticles in air. The photoactive layers were deposited inside a glove box (KIYON, KK-011AS-EXTRA) by spin-coating chloroform solutions containing PTB7-Th and the DTTB-based polymers. Optimal fabrication conditions were as follows: chloroform solutions of PTB7-Th:**P1** and PTB7-Th:**P2** (8 g L^{-1} total concentration) were prepared by stirring at 50 ℃ until complete dissolution. The p:n ratio was 1:1 (w/w). The solutions were cooled to room temperature and spin-coated at 1000 rpm for 10 s. The resulting thin films were transferred into a vacuum evaporator (ALS Technology, E-100J) connected to the glove box, where MoO_x (7.5 nm) and Ag (100 nm) layers were sequentially deposited through a shadow mask. The active area of the cells was 0.1256 cm^2, defined by a circular shadow mask with a radius of 2.0 mm. *J–V* characteristics were measured using a Keithley 2400 source-measure unit in the glove box under the 1 sun (AM1.5G) condition using a solar simulator (SAN-EI Electric, XES-40S1). The light intensity was calibrated with a silicon reference photovoltaic cell (Bunkoukeiki, BS520BK). EQE spectra were measured using a Spectral Response Measuring System (Bunkoukeiki, ECT-250DP). The photovoltaic properties were averaged over at least five substrates (each containing four photoactive areas). The thicknesses of the photoactive layers were measured using an ET4000 (Kosaka Laboratory, Ltd.); the optimal photoactive layer thickness was around 100 nm.

2D-GIXD measurements

Two-dimensional grazing-incidence X-ray diffraction (2D-GIXD) experiments were conducted at SPring-8 on beamline BL46XU. Samples were irradiated with an X-ray energy of 12.39 keV (λ = 1 Å) at a fixed incident angle on the order of 0.12° using a Huber diffractometer. The resulting 2D-GIXD patterns were recorded using a 2D image detector (Pilatus 300 K). Samples for the GIXD measurements were prepared following the same procedures used for OFETs and OPV devices.

Synthesis of (3-thienyl)disulfide

The synthesis was performed according to the reported procedure.[S3] To a solution of 3-bromothiophene (19.0 mL, 200 mmol) in 150 mL of diethyl ether, *n*BuLi (2.3 mol/L in cyclohexane, 86.9 mL, 200 mmol) was added dropwise at −78 °C. The reaction mixture was stirred for 1 h, followed by the addition of sulfur (6.43 g, 201 mmol). After stirring for 30 min, the mixture was allowed to warm to 0 °C and stirred for an additional 30 min. The reaction was quenched by the addition of 50 mL of water. Subsequently, an aqueous solution of $K_3[Fe(CN)_6]$ (1.0 M, 210 mL) was added dropwise, and the mixture was stirred at room temperature overnight. The organic layer was separated, washed twice with water, and then with brine. After drying over anhydrous $MgSO_4$, the solvent was removed under reduced pressure. The crude product was purified by silica gel chromatography using *n*-hexane as the eluent to afford bis(3-thienyl) disulfide (21.6 g, 93.8 mmol, 94% yield) as a yellow oil. ^{1}H NMR (500 MHz, $CDCl_3$) δ 7.34 (dd, J = 4.9, 3.0 Hz, 2H), 7.32 (dd, J = 3.0, 1.4 Hz, 2H), 7.12 (dd, J = 4.9, 1.4 Hz, 2H). The ^{1}H NMR data were consistent with the literature values.[S3]

Synthesis of compound 1

The synthesis was performed according to the reported procedure.[S4] To a solution of diisopropylamine (14.8 mL, 105 mmol) in 200 mL of THF, *n*BuLi (2.3 mol/L in cyclohexane, 43.5 mL, 100 mmol) was slowly added dropwise at −78 °C. The mixture was then warmed to 0 °C and stirred for 1 h to prepare LDA. After recooling the reaction mixture to −85 °C, a solution of 1,3-dibromobenzene (12.0 mL, 99.7 mmol) in 30 mL of THF was added slowly at a rate such that the internal temperature did not exceed −75 °C. After stirring for 2 h, chlorotrimethylsilane (12.6 mL, 99.7 mmol) was added, and the mixture was stirred overnight. The reaction was quenched with water, and the organic layer was separated, washed twice with water, and then with brine. After drying over anhydrous $MgSO_4$, the solvent was removed under reduced pressure. The crude product was purified by silica gel chromatography using *n*-hexane as the eluent to afford compound **1** (29.7 g, 96.4 mmol, 97% yield) as a colorless oil. ^{1}H NMR (400 MHz, $CDCl_3$) δ 7.51 (d, J = 7.9 Hz, 2H), 6.97 (t, J = 7.9 Hz, 1H), 0.57 (s, 9H). The ^{1}H NMR data were consistent with the literature values.[S4]

Synthesis of compound 2

To a solution of compound **1** (29.2 g, 94.8 mmol) in 150 mL of diethyl ether, *n*BuLi (2.66 mol/L in hexane, 35.9 mL, 95.5 mmol) was added dropwise at −78 ℃. The reaction mixture was stirred at this temperature for 1 h, followed by the addition of (3-thienyl)disulfide (22.0 g, 95.5 mmol) at –78 ℃. The mixture was then allowed to warm to room temperature and stirred overnight. After cooling to 0 ℃, the reaction mixture was quenched by the slow addition of 100 mL of water. An aqueous solution of $K_3[Fe(CN)_6]$ (1.0 M, 100 mL) was added, and the reaction mixture was stirred at room temperature for 1 h. The organic layer was separated, washed twice with water, then with brine. After drying over anhydrous magnesium sulfate, the solvent was removed under reduced pressure. The crude product was purified by silica gel chromatography using *n*-hexane as the eluent to afford compound **2** (32.0 g, 93.2 mmol, 98% yield) as a colorless oil. Bis(3-thienyl)disulfide (8.79 g, 38.2 mmol) was also recovered. ^{1}H NMR (400 MHz, $CDCl_3$) δ 7.39 (d, *J* = 7.8 Hz, 1H, Bz), 7.36 (dd, *J* = 4.9, 3.0 Hz, 1H, Th), 7.20 (d, *J* = 3.0 Hz, 1H, Th), 7.06 (d, *J* = 7.8 Hz, 1H, Bz), 6.98 (t, *J* = 7.8 Hz, 1H, Bz), 6.91 (d, *J* = 4.9 Hz, 1H, Th), 0.57 (s, 9H, $SiMe_3$). ^{13}C NMR (126 MHz, $CDCl_3$) δ 146.0, 140.5, 132.1, 131.4, 131.1, 130.3, 130.12, 130.06, 126.8, 126.4, 4.1. HR-MS (APCI) Calcd for $C_{13}H_{15}BrS_2Si$: M^+: 341.95623, Found: 341.95654.

Synthesis of compound 3

Compound **3** was prepared from compound **2** (16.0 g, 46.6 mmol), *n*BuLi (2.66 mol/L in hexane, 17.7 mL, 47.1 mmol), (3-thienyl)disulfide (10.8 g, 46.9 mmol) in 150 mL of diethyl ether, following a procedure similar to that described for compound **2**. The product was obtained as a white solid (10.7 g, 28.3 mmol, 61% yield). ^{1}H NMR (500 MHz, $CDCl_3$) δ 7.34 (dd, *J* = 5.0, 3.0 Hz, 2H), 7.16 (dd, *J* = 3.0, 1.3 Hz, 2H), 7.04–6.99 (m, 3H, Bz), 6.92 (dd, *J* = 5.0, 1.3 Hz, 2H, Th), 0.57 (s, 9H, $SiMe_3$). ^{13}C NMR (126 MHz, $CDCl_3$) δ 144.7, 141.3, 132.1, 130.0, 129.7, 126.7, 125.7, 4.36. HR-MS (APCI) Calcd for $C_{17}H_{18}S_4Si$: M^+: 378.00551, Found: 378.00519. m.p. 125.0-126.1 ℃.

Synthesis of compound 4

To a solution of compound **3** (5.64 g, 14.9 mmol) in 300 mL of dichloromethane, NBS (8.75 g, 49.2 mmol)

was added in several portions at room temperature. The mixture was stirred overnight, then quenched with water. The organic layer was separated, and the aqueous layer was extracted with 100 mL of dichloromethane. The combined organic layers were washed with brine and dried over anhydrous magnesium sulfate. After evaporation of the solvent, the resulting solid was washed with ethanol to afford compound **4** (7.15 g, 13.2 mmol, 89% yield) as a white solid. ^{1}H NMR (400 MHz, $CDCl_3$) δ 7.37 (d, J = 5.6 Hz, 2H, Th), 7.03–6.93 (m, 3H, Th and Bz), 6.45 (d, J = 7.9 Hz, 2H, Bz). ^{13}C NMR (126 MHz, $CDCl_3$) δ 139.5, 132.5, 129.1, 127.8, 127.1, 123.9, 121.0, 118.8. HR-MS (APCI) Calcd for $C_{14}H_7Br_3S_4$: M^+: 539.69752, Found: 539.69885. m.p. 175.2-176.8 ℃.

Synthesis of DTTB

To a solution of compound **4** (520 mg, 0.957 mmol) in 14 mL of CPME, *n*BuLi (2.3 mol/L in cyclohexane, 1.25 mL, 2.89 mmol) was added dropwise at −78 ℃. The reaction mixture was stirred at this temperature for 1 h, followed by the addition of trimethyl borate (0.107 mL, 0.958 mmol) at –78 ℃. The mixture was then heated at 60 °C and stirred overnight. The reaction was quenched with saturated aqueous NH_4Cl, and the aqueous layer was extracted with dichloromethane. After drying over anhydrous magnesium sulfate, the solvent was removed under reduced pressure. The resulting solid was washed with ethanol and recrystallized from toluene to afford **DTTB** (180 mg, 0.573 mmol, 60% yield) as yellow needle-like crystals. ^{1}H NMR (400 MHz, $CDCl_3$) δ 8.00 (d, J = 5.0 Hz, 2H, Th), 7.60 (dd, J = 7.8, 0.8 Hz, 2H, Bz), 7.54–7.48 (m, 1H, Bz), 7.37 (d, J = 5.0 Hz, 2H, Th). ^{13}C NMR (101 MHz, $CDCl_3$) δ 143.4, 143.2, 135.2, 128.8, 125.6, 122.2. The two C–B carbon signals were not observed due to quadrupolar interaction.^{11}B NMR (160 MHz, $CDCl_3$) δ 36.8. HR-MS (APCI) Calcd for $C_{14}H_7BS_4$: M^+: 313.95209, Found: 313.95221. m.p. 204.5-206.8 ℃.

Synthesis of DTTB-Sn

LiTMP was prepared according to the reported procedure.[S5] To a solution of **DTTB** (315 mg, 1.00 mmol) in 20 mL of THF, LiTMP (0.640 mol/L in THF, 6.40 mL, 4.10 mmol) was added dropwise at −78 ℃. The reaction mixture was stirred at this temperature for 1 h, followed by the addition of trimethyltin chloride (1.00 mol/L in hexane, 4.00 mL, 4.00 mmol) at –78 ℃. The mixture was allowed to warm to room temperature and stirred

for an additional 2 h. The reaction was quenched with water, and the aqueous layer was extracted with 100 mL of dichloromethane. After drying over anhydrous magnesium sulfate, the solvent was removed under reduced pressure. The residue was dissolved in methanol and extracted with hexane (20 mL × 3). Removal of the solvent under reduced pressure gave the crude product (337 mg, 53%). Recrystallization from toluene/ethanol afforded the analytically pure product as a yellow solid (230 mg, 0.359 mmol, 36% yield). ^{1}H NMR (400 MHz, $CDCl_3$) δ 7.58 (d, *J* = 7.5 Hz, 2H, Bz), 7.51–7.37 (m, 3H, Th and Bz), 0.49 (s, 18H, $SnMe_3$). ^{13}C NMR (126 MHz, $CDCl_3$) δ 150.2, 143.5, 143.3, 138.6 (br, B–C), 132.7, 128.6, 128.2 (br, B–C), 122.0, -8.0. ^{11}B NMR (160 MHz, $CDCl_3$) δ 36.1. HR-MS (APCI) Calcd for $C_{20}H_{23}BS_4Sn_2$: M^+: 641.88180, Found: 641.88208. m.p. 188.0-191.2 ℃.

Synthesis of DTTB-NPh

A mixture of **DTTB-Sn** (159 mg, 0.248 mmol), 4-bromotriphenylamine (177 mg, 0.546 mmol), XPhos (4.3 mg, 9.0 μmol, 3.5 mol%), and $Pd(dba)_2$ (3.6 mg, 6.3 μmol, 2.5 mol%) in 15 mL of toluene was stirred at 110 °C overnight. The resulting mixture was quenched with water, and the organic layer was separated. The aqueous layer was extracted with toluene, and the combined organic layers were washed with water and brine. After drying over anhydrous magnesium sulfate, the solvent was evaporated. The residue was purified by recrystallization from toluene/ethanol to afford **DTTB-NPh** (99.0 mg, 0.124 mmol, 50% yield) as a yellow solid. ^{1}H NMR (400 MHz, $CDCl_3$) δ 7.66 (d, *J* = 8.5 Hz, 4H, phenylene), 7.56 (d, *J* = 7.6 Hz, 2H, Bz), 7.49–7.42 (m, 3H, Th and Bz), 7.30 (t, *J* = 8.0 Hz, 8H, Ph), 7.16 (d, *J* = 8.0 Hz, 8H, Ph), 7.13–7.04 (m, 8H, Ph and phenylene). ^{13}C NMR (101 MHz, $CDCl_3$) δ 153.7, 148.6, 147.2, 144.1, 143.0, 131.7, 129.4, 128.5, 127.4, 124.9, 123.6, 122.9, 122.2, 120.3. The two C–B carbon signals were not observed due to quadrupolar interaction. ^{11}B NMR (160 MHz, $CDCl_3$) δ 34.3. HR-MS (APCI) Calcd for $C_{50}H_{33}BN_2S_4$: M^+: 800.16226, Found: 800.16125. m.p. >300 ℃.

Synthesis of P1

A mixture of **DTTB-Sn** (100 mg, 0. 156 mmol), **NDI-Br** (154 mg, 0.156 mmol), XPhos (2.2 mg, 4.6 μmol, 3 mol%), and $Pd(dba)_2$ (2.2 mg, 3.8 μmol, 2.5 mol%) in 20 mL of toluene was stirred at 110 °C for 72 h. The

mixture was cooled to room temperature and quenched with water. The organic layer was separated, and the aqueous layer was extracted with chloroform. The combined organic layers were washed with water and brine. After drying over anhydrous magnesium sulfate, the solvent was evaporated. The residue was purified by passage through a silica pad with chloroform followed by reprecipitation from chloroform/ethanol to yield **P1** (73.0 mg, 41%) as a black powder. ^{1}H NMR (400 MHz, $CDCl_3$) δ 9.94–6.11 (m, 7H, aromatic), 4.90–2.54 (m, 4H, N-CH_2), 2.23–0.54 (m, 78H). ^{11}B NMR (160 MHz, $CDCl_3$, at 50 °C) δ 25.4. m.p. 248.6-249.8℃.

Synthesis of P2

P2 was prepared from **DTBB-Sn** (200 mg, 0.313 mmol), **DPP-Br** (389 mg, 0.313 mmol), XPhos (4.5 mg, 9.4 μmol, 3 mol%), and $Pd(dba)_2$ (5.4 mg, 9.4 μmol, 3 mol%) in 20 mL of toluene, following a procedure similar to that for **P1**. After purification by reprecipitation from chloroform/ethanol, **P2** (358 mg, 82%) was obtained as a black powder. ^{1}H NMR (500 MHz, $CDCl_3$, at 50 °C) δ 9.60–6.58 (m, 9H, aromatic), 4.67–3.52 (m, 4H, N-CH_2), 2.18–0.74 (m, 110H, alkyl). ^{11}B NMR (160 MHz, $CDCl_3$, at 50 °C) δ 27.2. m.p. 278.2-279.8℃.

Figures and Tables

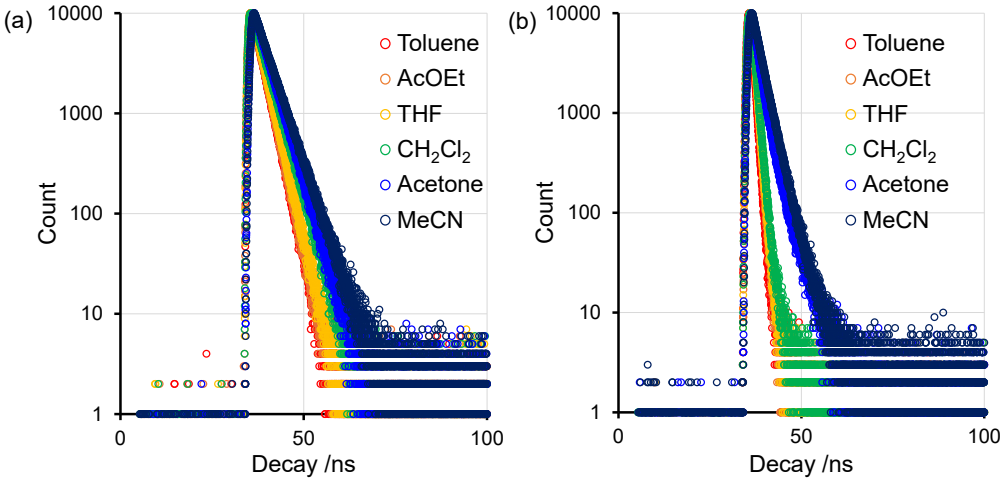

Figure S1 Fluorescence decays of **DTTB** (a) and **DTTB-NPh** (b) in solution at r.t.

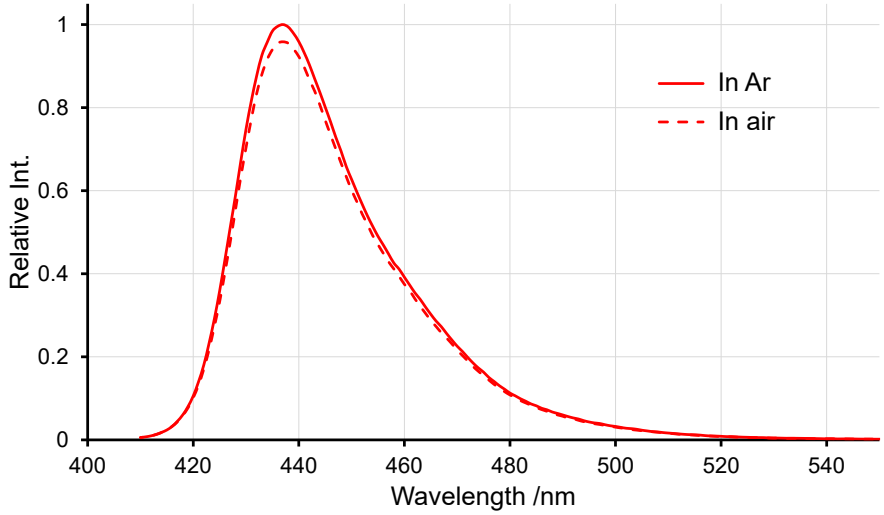

Figure S2 PL spectra of **DTTB** in toluene at r.t. The PL spectra are normalized to an intensity of 1.0 at the PL maximum in argon.

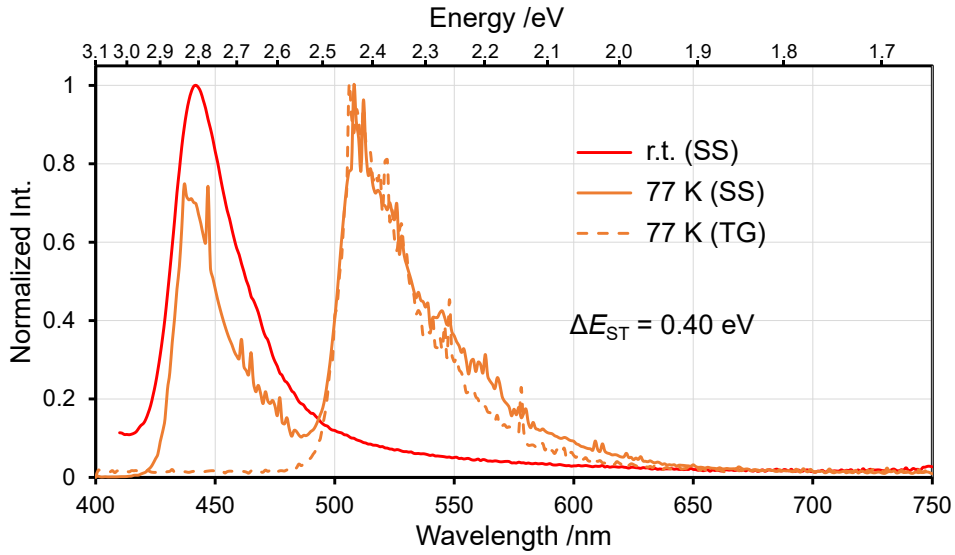

Figure S3 Steady-state (SS) and time-gated (TG) PL spectra of **DTTB** in a PMMA matrix (1 wt%) at room temperature and 77 K.

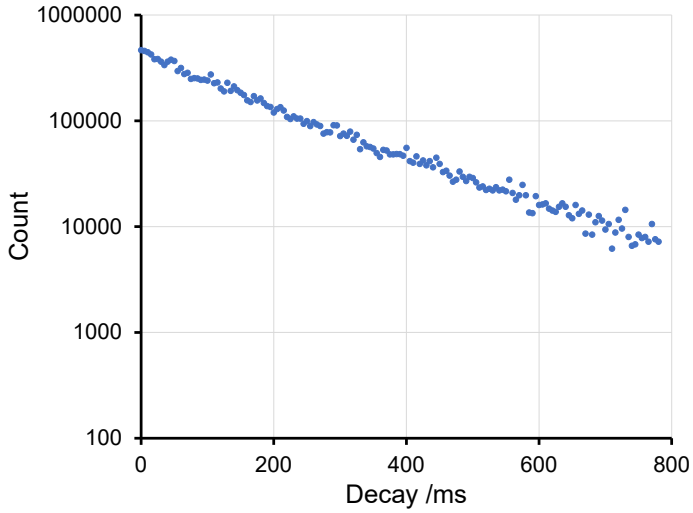

Figure S4 PL decay curve of **DTTB** in a PMMA matrix (1 wt%) at 77 K.

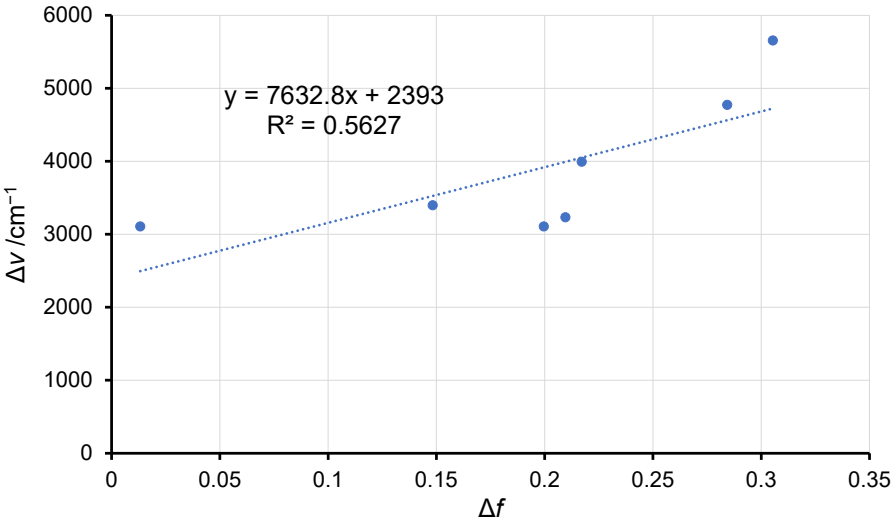

Figure S5 Lippert-Mataga plot of **DTTB-NPh** in various solvents.

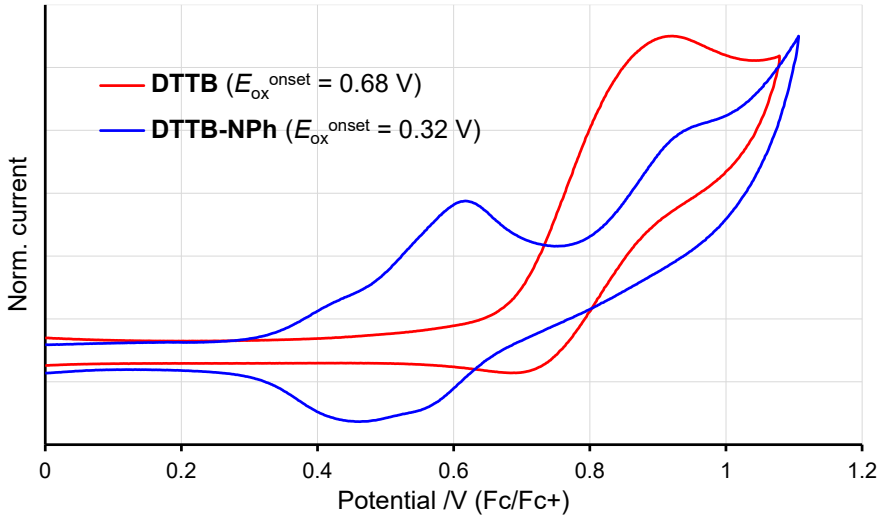

Figure S6 Anodic cyclic voltammetry data of **DTTB** and **DTTB-NPh** in dichloromethane containing 0.1 M Bu_4NPF_6 at the scan rate of 100 mV s^{-1}.

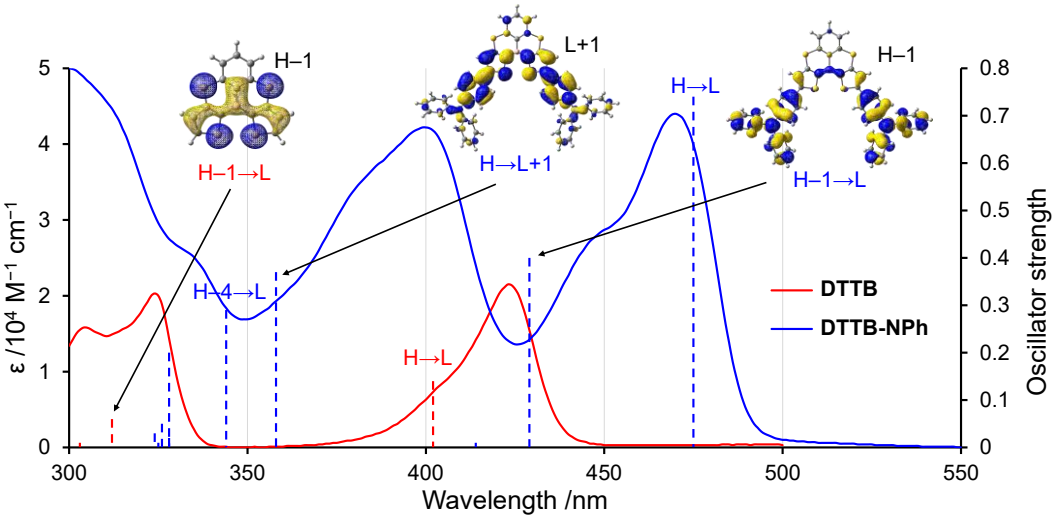

Figure S7 Experimental absorption spectra and TD-DFT calculation results of **DTTB** and **DTTB-NPh**. H and L denote HOMO and LUMO, respectively. The HOMO and LUMO are shown in Figure 5.

Table S1 Main results of TD-DFT calculations for **DTTB** and **DTTB-NPh**. Transitions with oscillator strengths lower than 0.03 are excluded. H and L denote HOMO and LUMO, respectively.

Compound	Excited State	Composition	Composition /%	Excitation energy /eV	Wavelength /nm	Oscillator strength
DTTB	$S_0 \rightarrow S_1$	H→L	98	3.08	402	0.14
	$S_0 \rightarrow S_2$	H-1→L	93	3.97	312	0.06
		H→L+1	5			
	$S_0 \rightarrow S_4$	H-4→L	2	4.18	297	0.12
		H-2→L	38			
		H→L+2	57			
	$S_0 \rightarrow S_5$	H-3→L	8	4.20	295	0.07
		H-1→L	5			
		H→L+1	84			
	$S_0 \rightarrow S_6$	H-3→L	82	4.46	278	0.13
		H-1→L+2	3			
		H→L+1	7			
		H→L+3	5			
	$S_0 \rightarrow S_8$	H-4→L	95	4.78	260	0.05
DTTB-NPh	$S_0 \rightarrow S_1$	H→L	98	2.61	475	0.74
	$S_0 \rightarrow S_2$	H-1→L	99	2.89	429	0.40
	$S_0 \rightarrow S_4$	H→L+1	96	3.47	358	0.37
	$S_0 \rightarrow S_5$	H-4→L	3	3.61	344	0.29
		H-1→L+1	93			
	$S_0 \rightarrow S_7$	H-3→L	4	3.79	328	0.20
		H-2→L+1	92			
	$S_0 \rightarrow S_8$	H-4→L	77	3.81	326	0.05
		H-1→L+1	2			
		H-1→L+4	4			
		H→L+2	3			
		H→L+3	9			

Table S2 Calculated NICS values.

Compound	Ring A		Ring B	
	NICS(1)	$NICS(1)_{zz}$	NICS(1)	$NICS(1)_{zz}$
DTTB	–2.14	0.35	–9.37	–21.48
DTCB	–0.34	4.90	–9.52	–22.25
DTSB	–4.44	–8.65	–9.88	–23.55

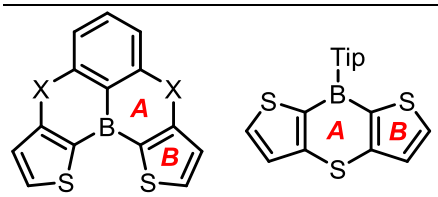

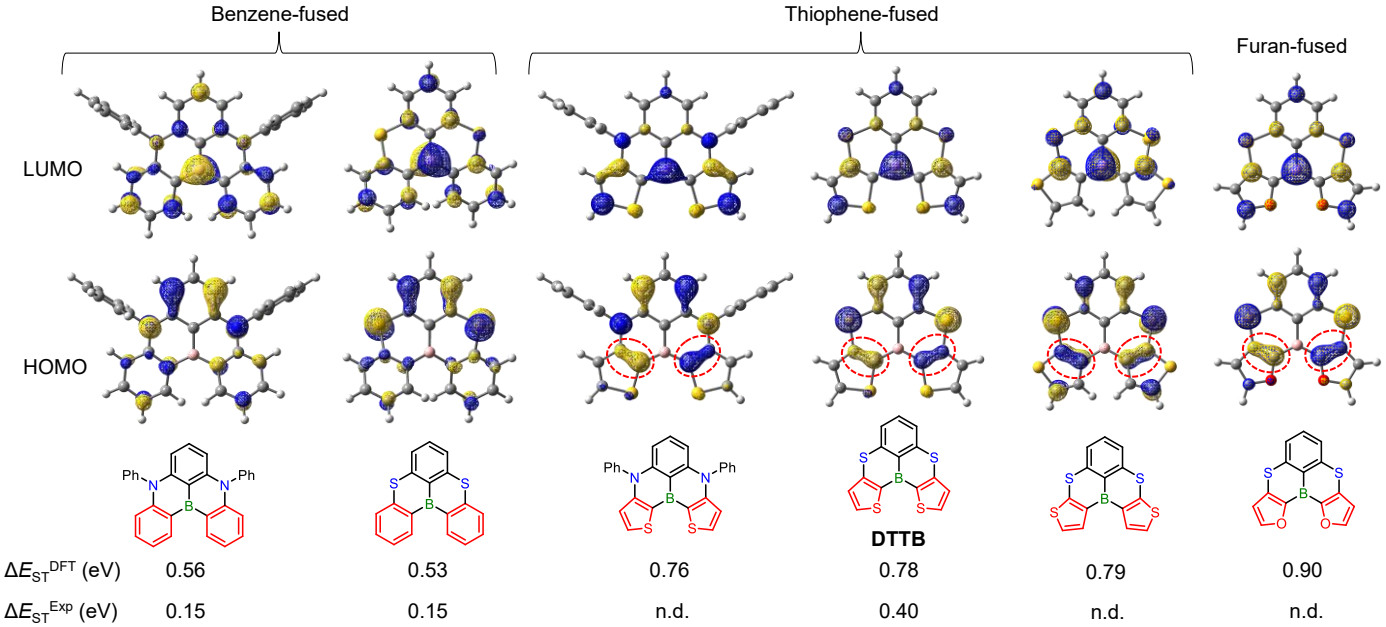

Figure S8 Frontier molecular orbitals (isovalue = 0.05) and ΔE_{ST} values of aromatic-fused planarized boranes. Experimental ΔE_{ST} values (ΔE_{ST}^{Exp}) were cited from the literature.[S6]

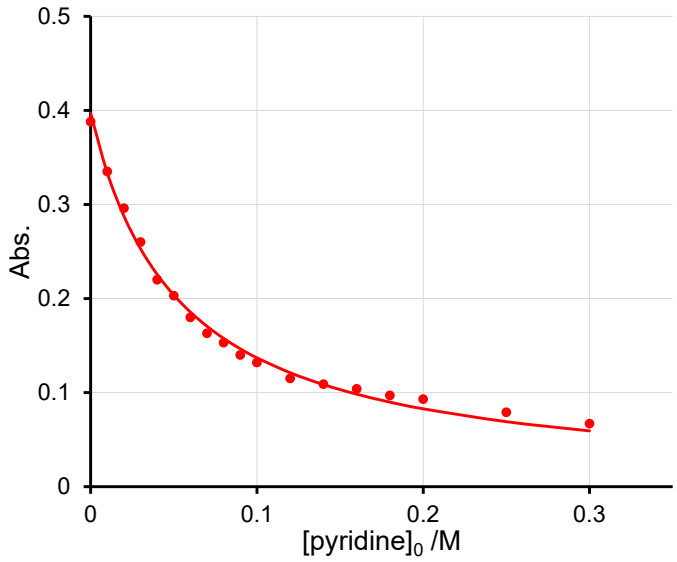

Figure S9 Titration curve of **DTTB** with pyridine at 423 nm (R^2 = 0.99457).

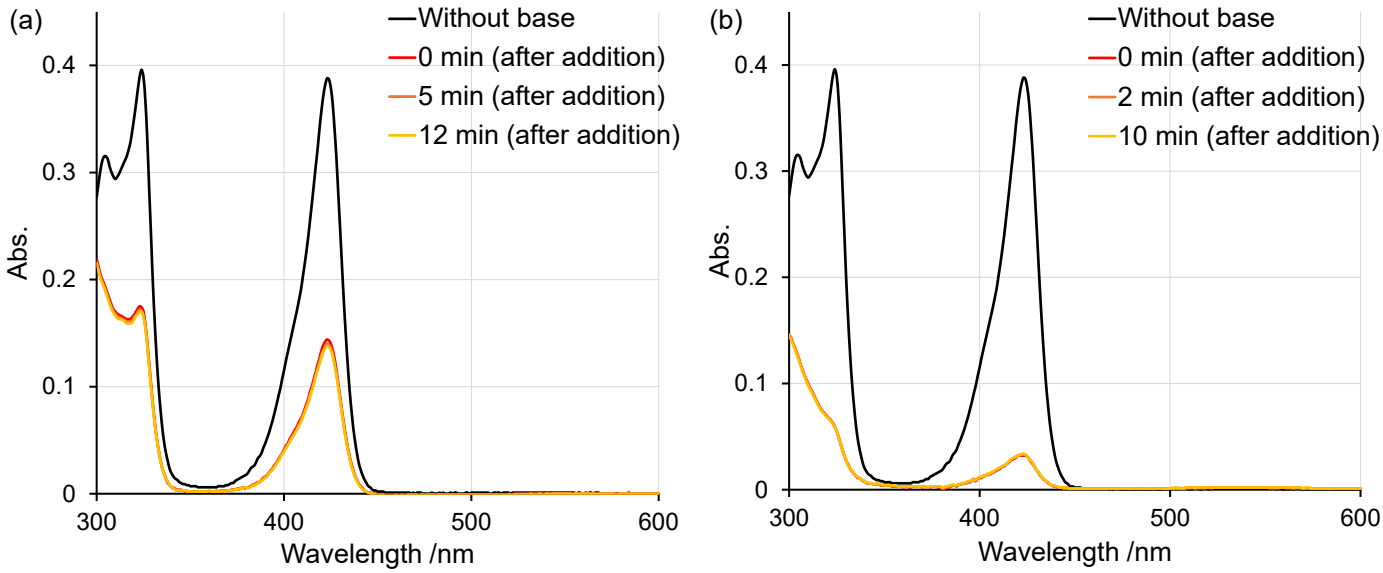

Figure S10 Time-dependent changes in the UV-vis spectra of **DTTB** (0.02 mM) upon the addition of (a) 0.1 M pyridine in toluene and (b) 1 equiv. of TBAF in THF.

Table S3 Calculated FIA values for triarylboranes.

Compound	FIA /kJ/mol
$B(C_6F_5)_3$	449
DTTB	281
DTCB	276
DTSB	283

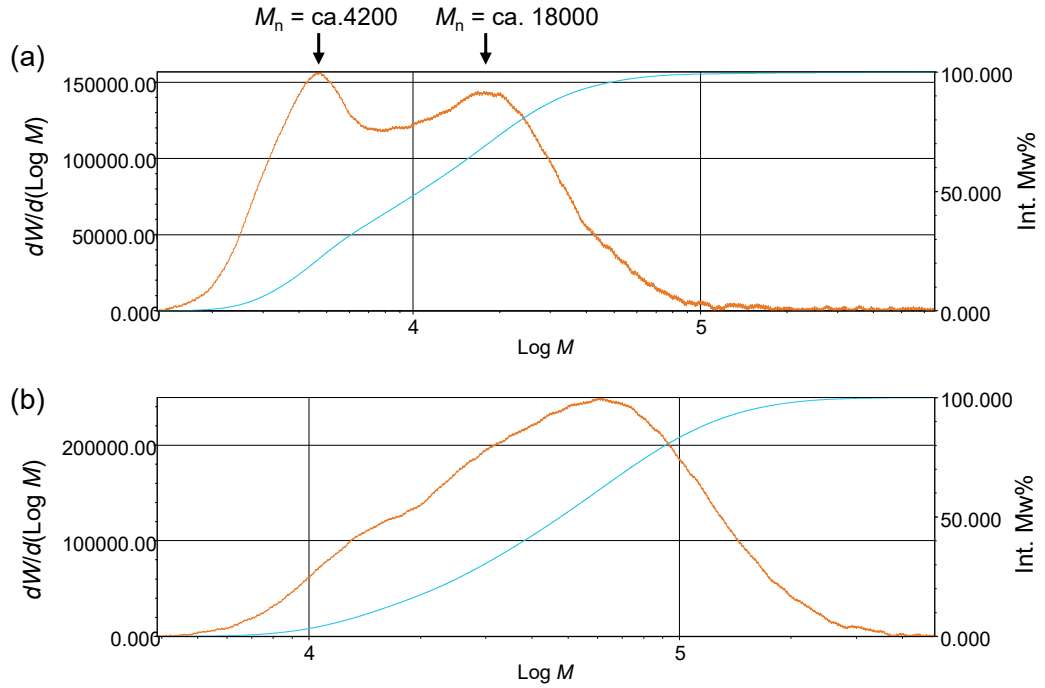

Figure S11 Molecular weight distributions of (a) **P1** and (b) **P2** determined by GPC.

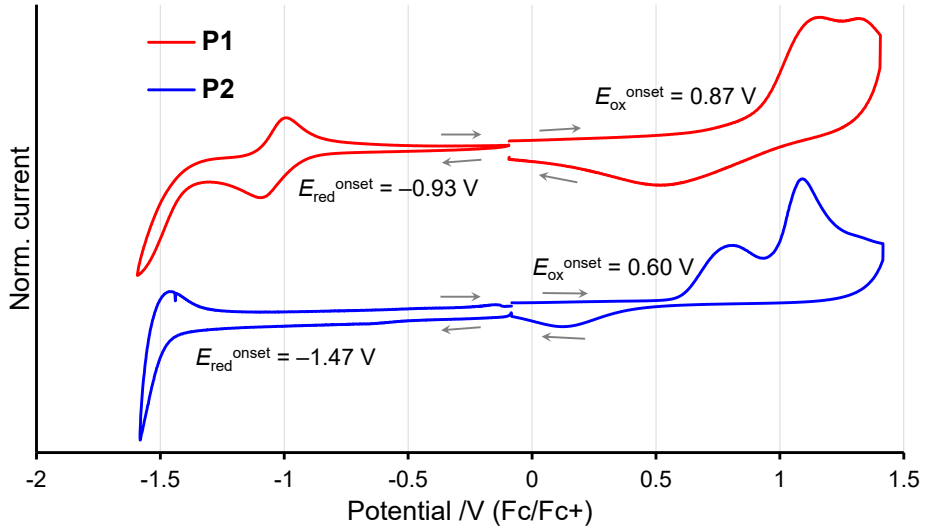

Figure S12 Cyclic voltammetry data of drop-casted films of **P1** and **P2** in acetonitrile containing 0.1 M Bu_4NPF_6 at the scan rate of 100 mV s^{-1}.

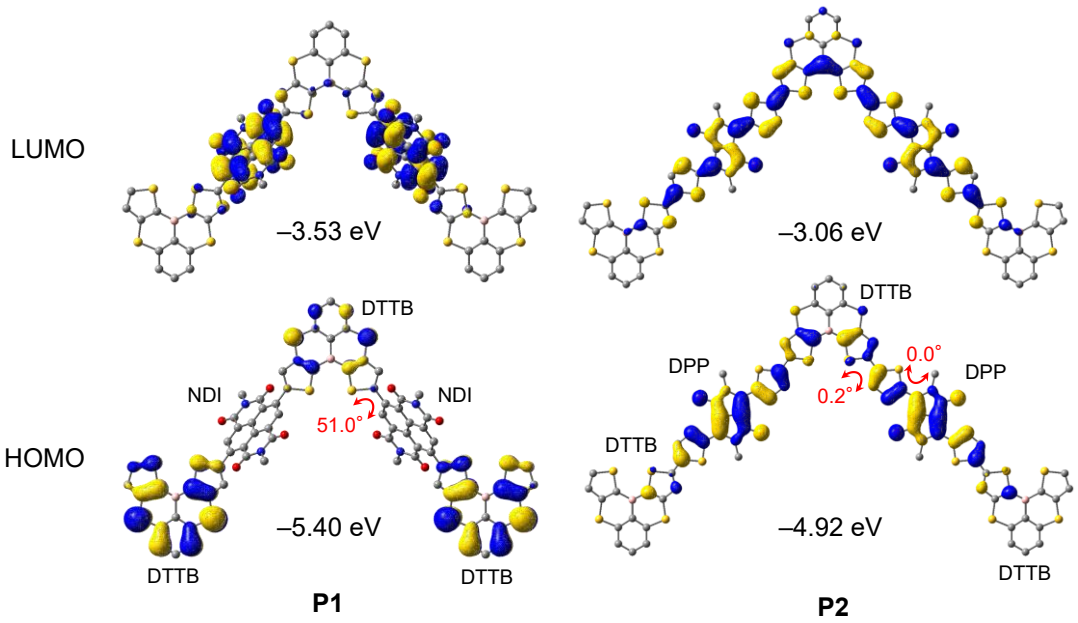

Figure S13 Frontier molecular orbitals of the oligomer models for **P1** and **P2**.

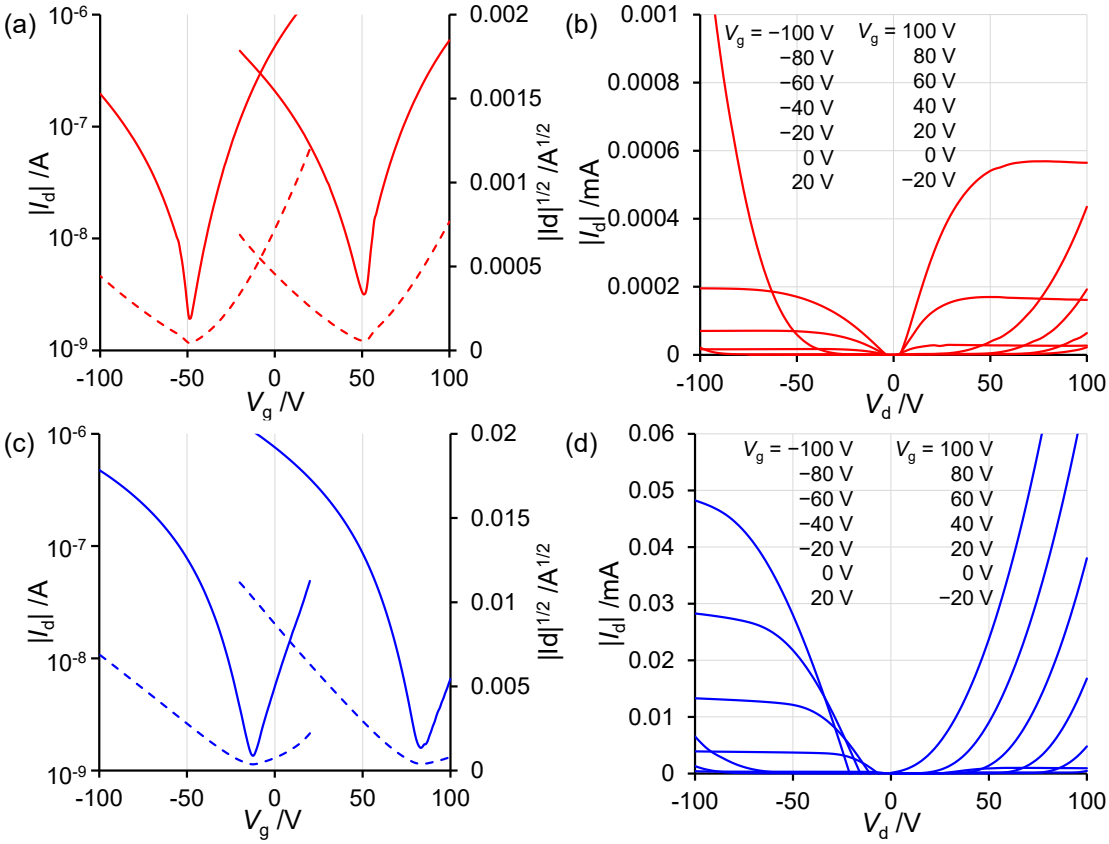

Figure S14 (a, c) Transfer and (b, d) output curves of the OFET devices: (a) and (b) **P1**; and (c) and (d) **P2**.

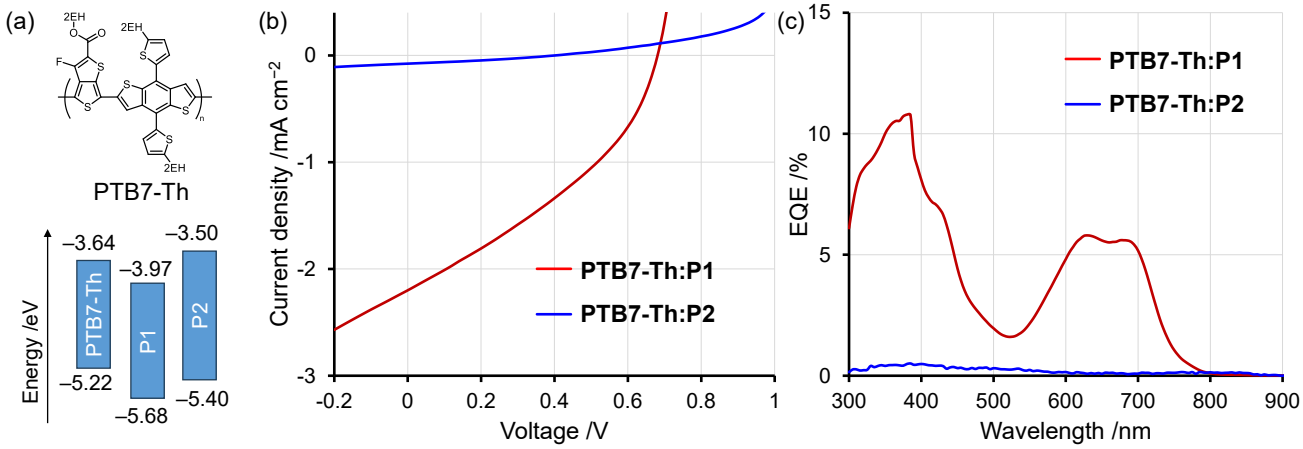

Figure S15 (a) *J*–*V* curves and (b) EQE spectra of all-polymer OPVs. The HOMO/LUMO energy levels of PTB7-Th were cited from the literature.[S7]

Table S4 Photovoltaic Properties of all-polymer OPVs.

Polymer	J_{SC} /mA cm^{-2}	V_{OC} /V	FF	PCE [PCE_{ave}] (%)[b]
P1	2.2 [1.1][a]	0.68	0.36	0.54 [0.51]
P2	0.09 [0.2][a]	0.4	0.31	0.01 [0.005]

[a] J_{SC} calculated from the EQE spectrum. [b] PCE: maximum power conversion efficiency. PCE_{ave}: average power conversion efficiency of more than 5 different cells under the same condition.

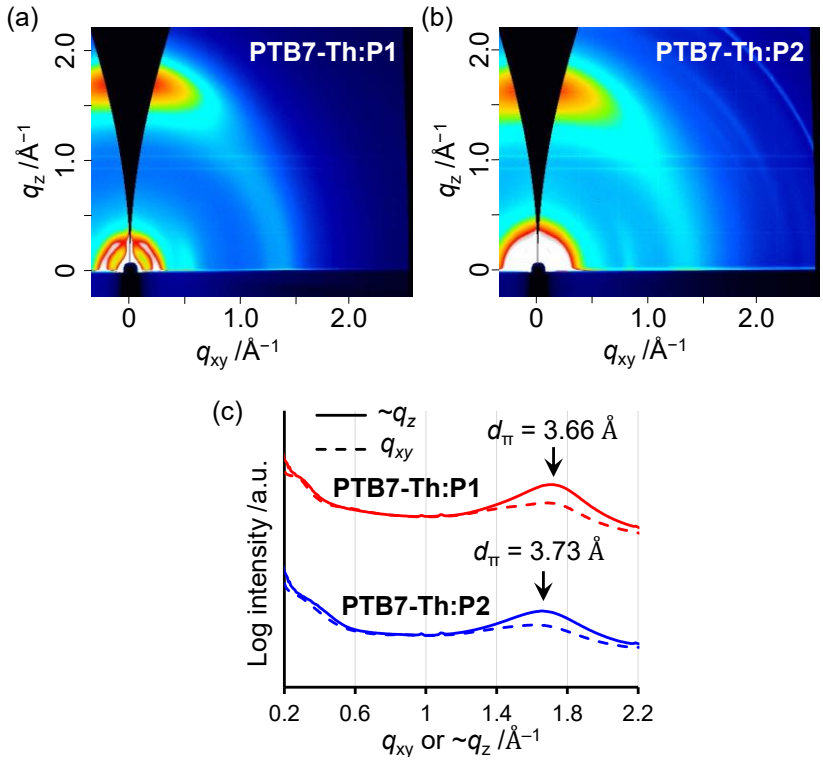

Figure S16 2D GIXD patterns of the PTB7-Th:polymer blend films for **P1** (a) and for **P2** (b). (c) Cross-sectional diffraction profiles cut from the 2D GIXD patterns along the q_{xy} (solid line) and ~q_z (dashed line) axes.

References

[S1] N. R. Kakde, H. Sharma, N. V. Dalvi, K. Vanka and A. S.K, *ACS Polym. Au*, 2024, **4**, 449.

[S2] B. Dyaga, A. Lemaire, S. Guchait, H. Zeng, B. Schmaltz and M. Brinkmann, *J. Mater. Chem. C*, 2023, **11**, 16554.

[S3] O. V. Borshchev, M. S. Skorotetcky, V. A. Trukhanov, R. S. Fedorenko, N. M. Surin, E. A. Svidchenko, A. Y. Sosorev, M. S. Kazantsev, D. Y. Paraschuk and S. A. Ponomarenko, *Dyes Pigm.*, 2021, **185**, 108911.

[S4] F. Mongin, E. Marzi and M. Schlosser, *Eur. J. Org. Chem.*, 2001, 2771.

[S5] R. E. Reddy and C. J. Kowalski, *Org. Synth.*, 1993, **71**, 146.

[S6] (a) T. Hatakeyama, K. Shiren, K. Nakajima, S. Nomura, S. Nakatsuka, K. Kinoshita, J. Ni, Y. Ono and T. Ikuta, *Adv. Mater.*, 2016, **28**, 2777; (b) F. Chen, L. Zhao, X. Wang, Q. Yang, W. Li, H. Tian, S. Shao, L. Wang, X. Jing and F. Wang, *Sci. China Chem.*, 2021, **64**, 547.

[S7] Y.-C. Lin, Y.-W. Su, J.-X. Li, B.-H. Lin, C.-H. Chen, H.-C. Chen, K.-H. Wu, Y. Yang and K.-H. Wei, *J. Mater. Chem. A*, 2017, **5**, 18053.

NMR spectra

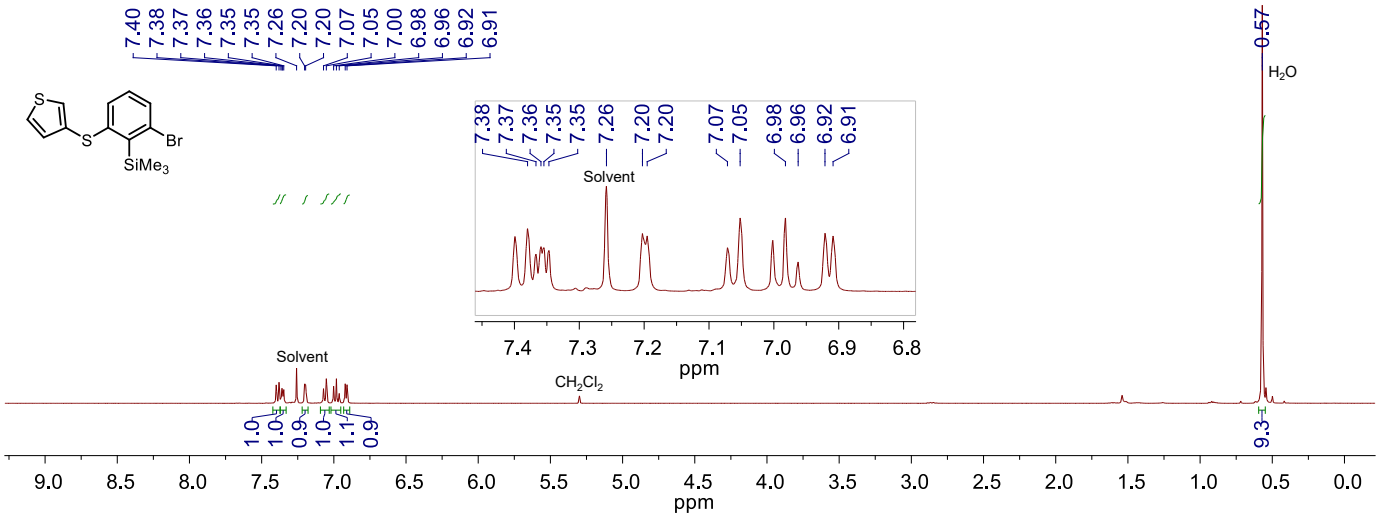

Figure S17 ^{1}H NMR spectrum of compound **2** in $CDCl_3$ at room temperature (400 MHz).

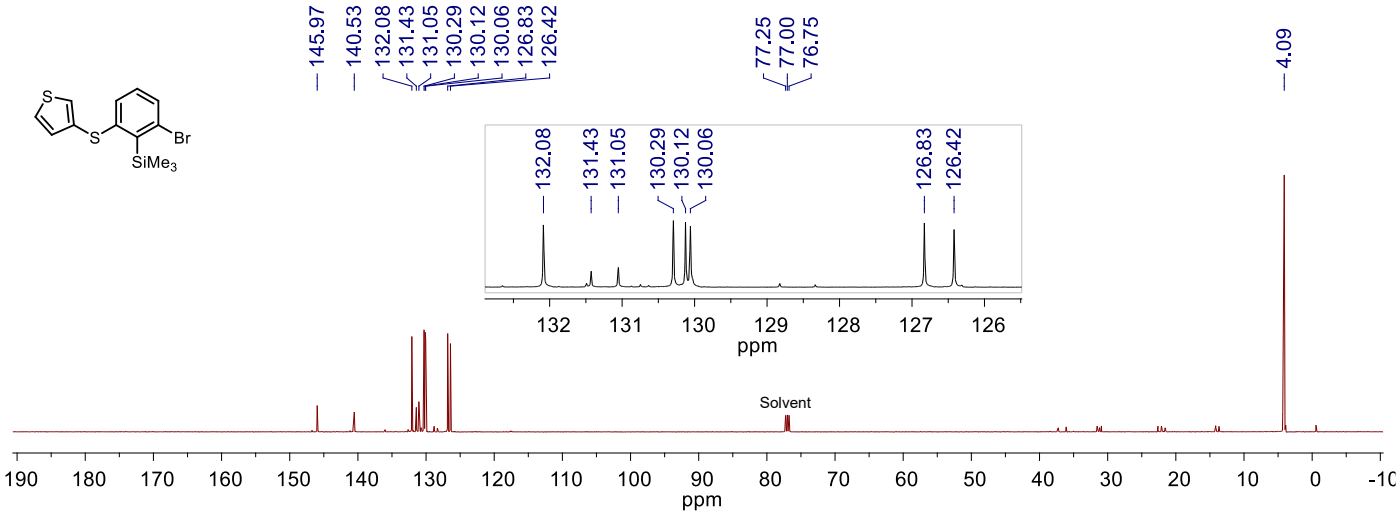

Figure S18 ^{13}C NMR spectrum of compound **2** in $CDCl_3$ at room temperature (126 MHz).

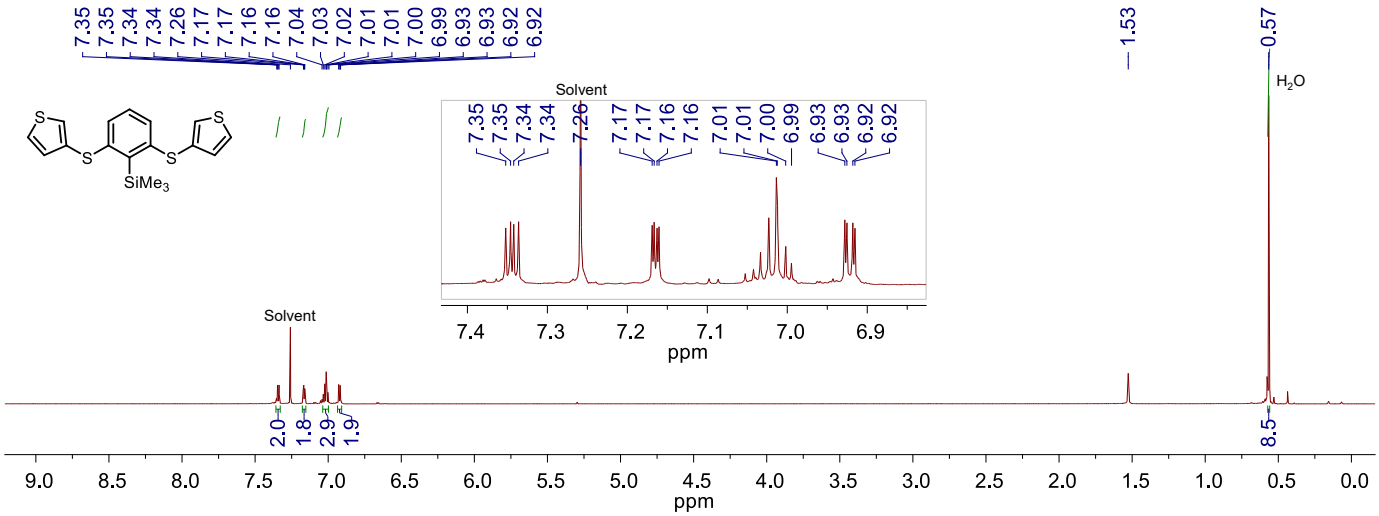

Figure S19 ^{1}H NMR spectrum of compound **3** in $CDCl_3$ at room temperature (500 MHz).

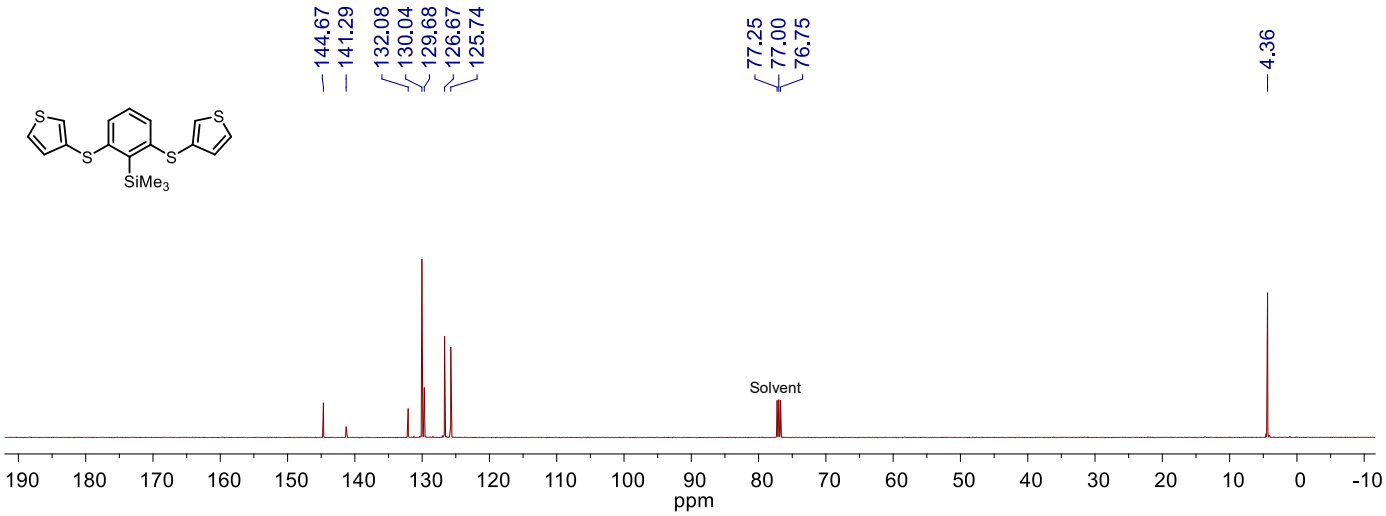

Figure S20 ^{13}C NMR spectrum of compound **3** in $CDCl_3$ at room temperature (126 MHz).

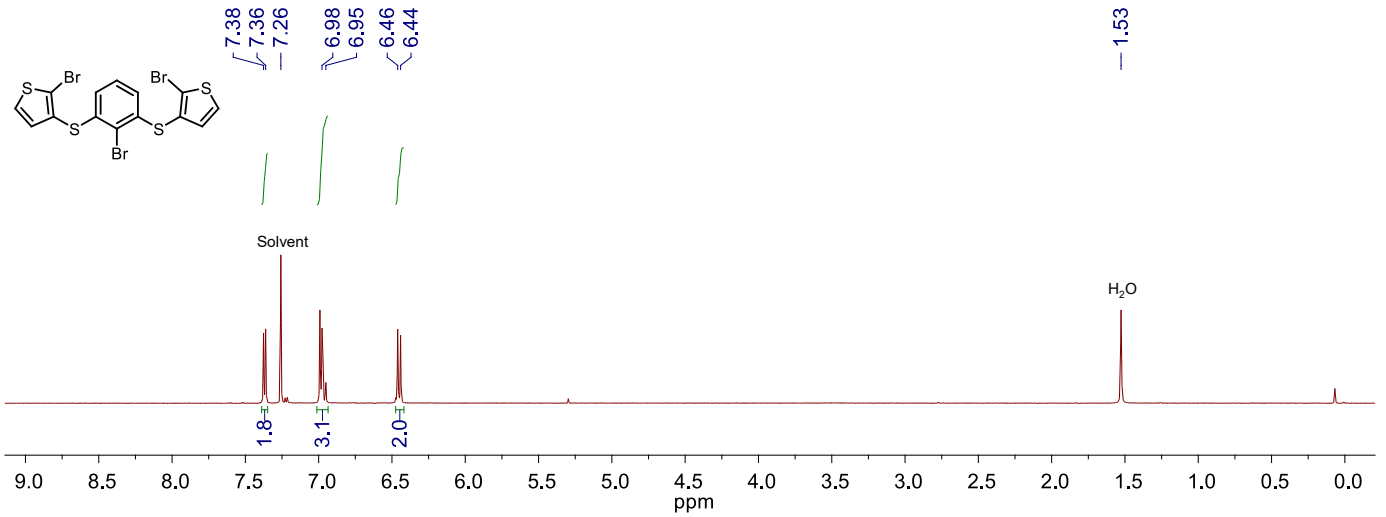

Figure S21 ^{1}H NMR spectrum of compound **4** in $CDCl_3$ at room temperature (400 MHz).

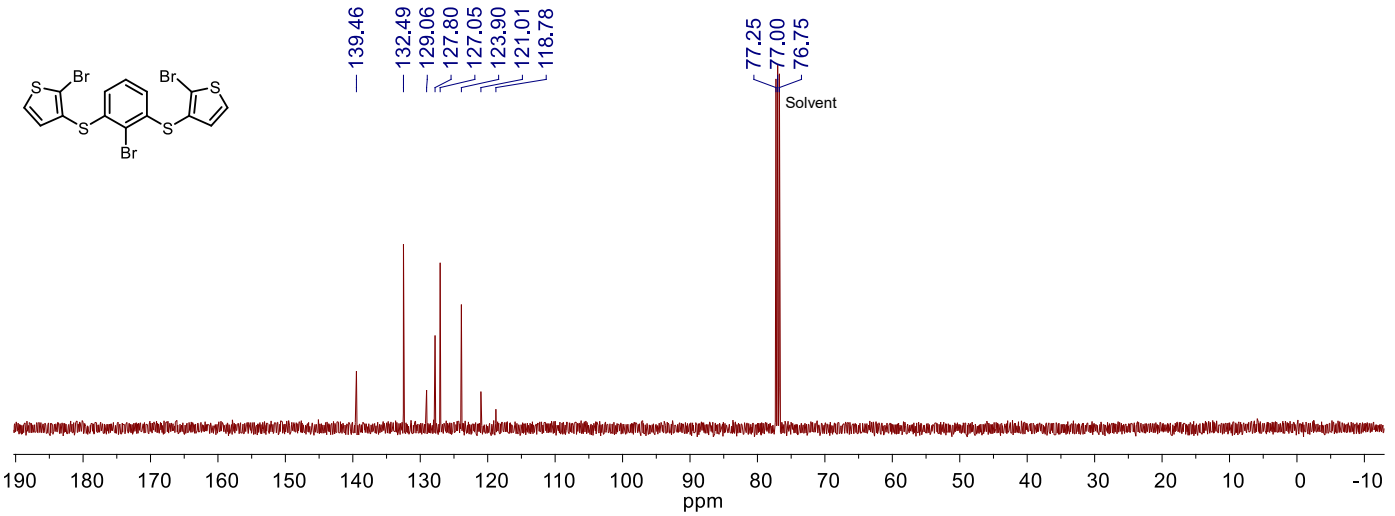

Figure S22 ^{13}C NMR spectrum of compound **4** in $CDCl_3$ at room temperature (126 MHz).

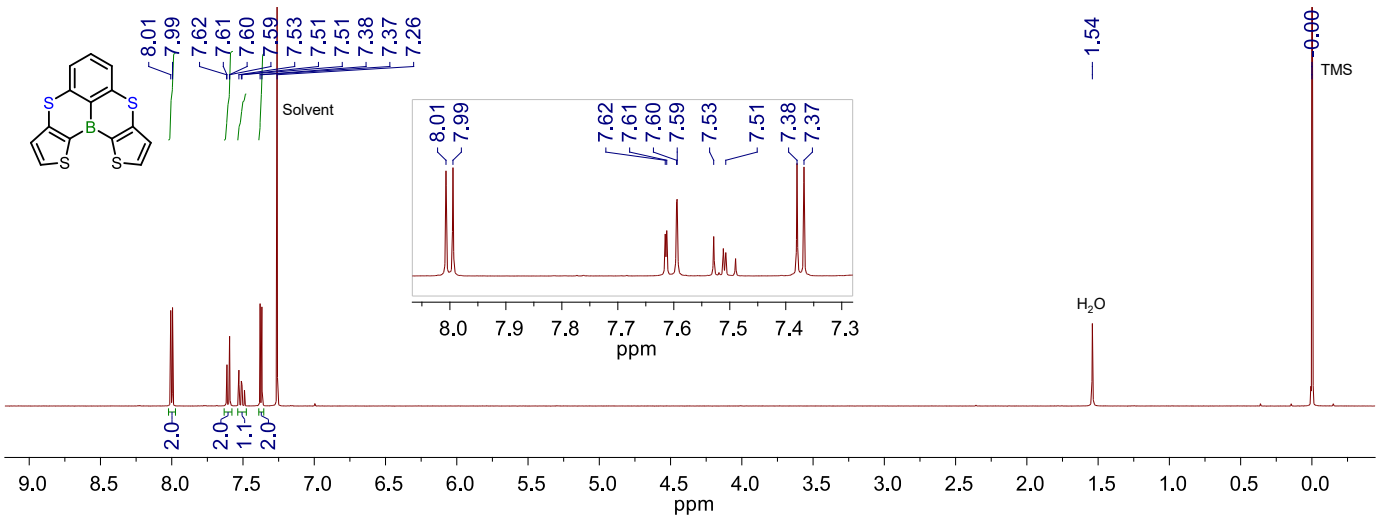

Figure S23 ^{1}H NMR spectrum of **DTTB** in $CDCl_3$ at room temperature (400 MHz).

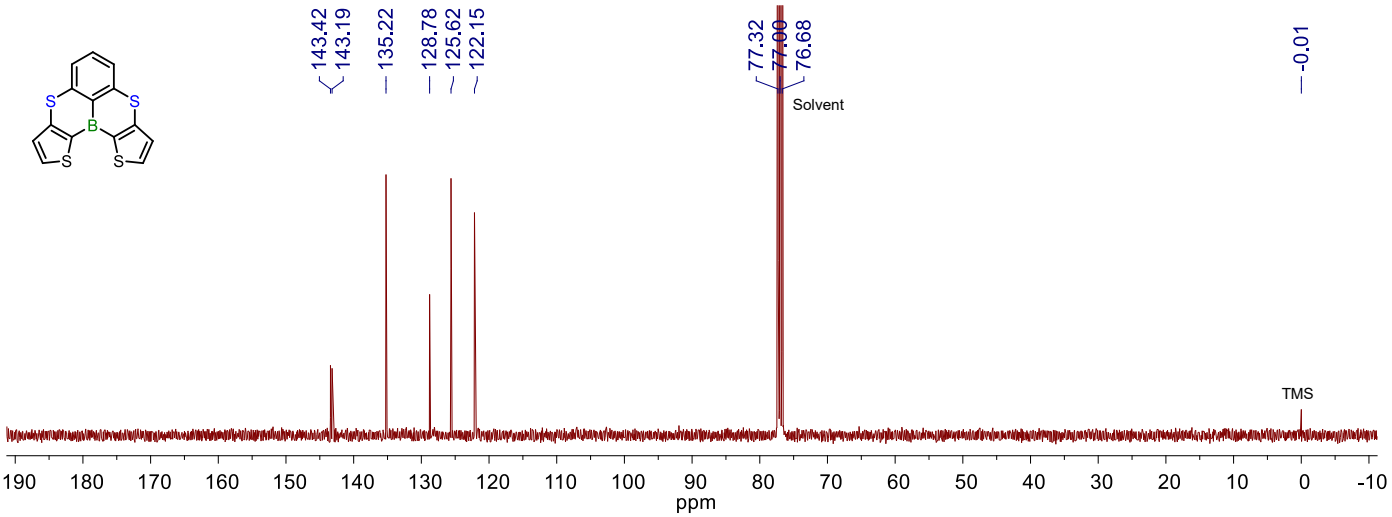

Figure S24 ^{13}C NMR spectrum of **DTTB** in $CDCl_3$ at room temperature (101 MHz).

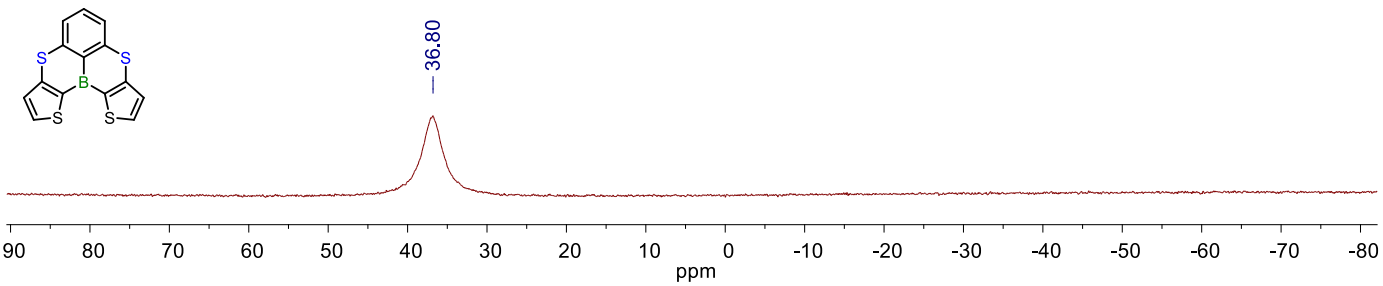

Figure S25 ^{11}B NMR spectrum of **DTTB** in $CDCl_3$ at room temperature (160 MHz).

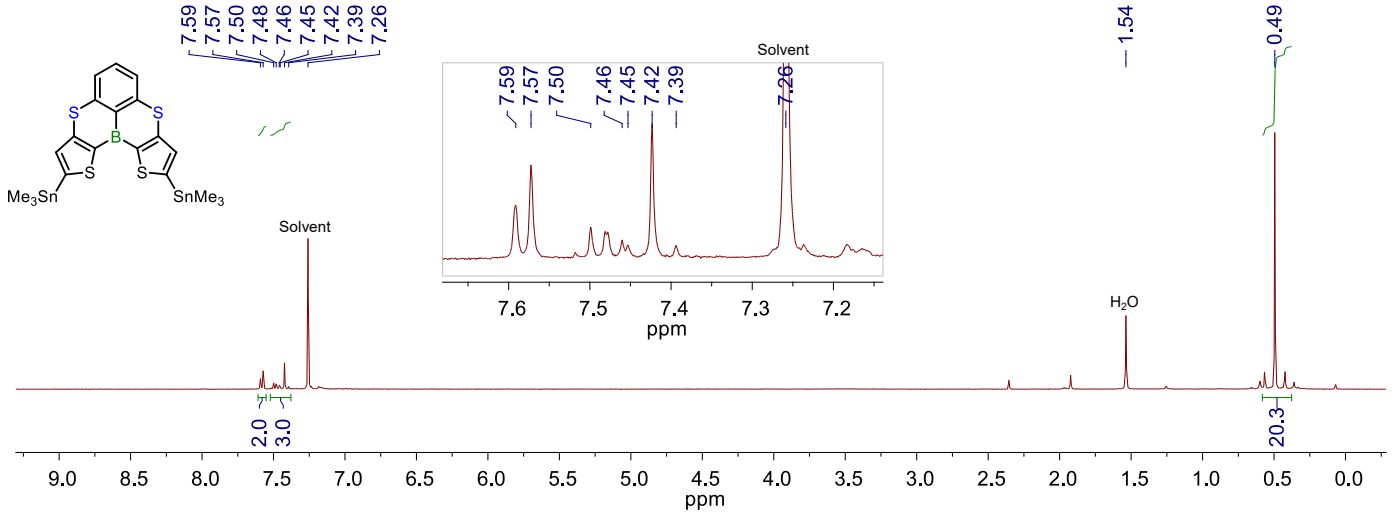

Figure S26 ^{1}H NMR spectrum of **DTTB-Sn** in $CDCl_3$ at room temperature (400 MHz).

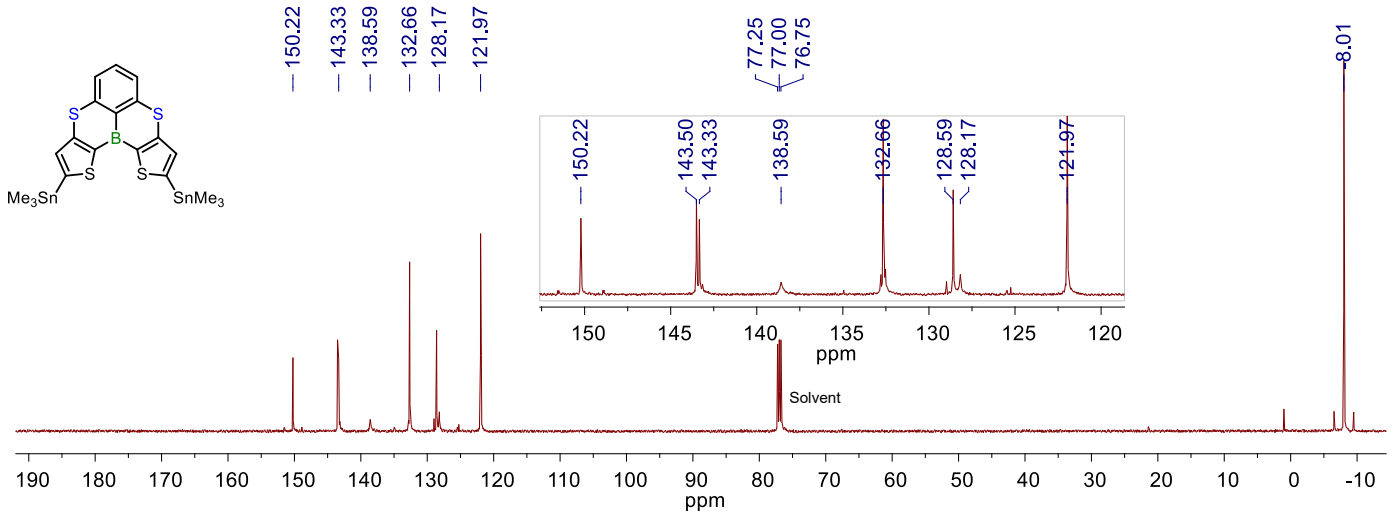

Figure S27 ^{13}C NMR spectrum of **DTTB-Sn** in $CDCl_3$ at room temperature (126 MHz).

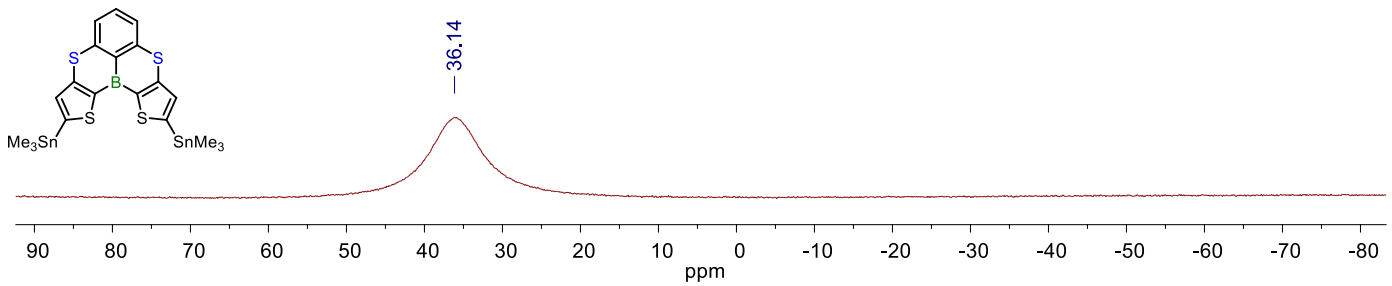

Figure S28 ^{11}B NMR spectrum of **DTTB-Sn** in $CDCl_3$ at room temperature (160 MHz).

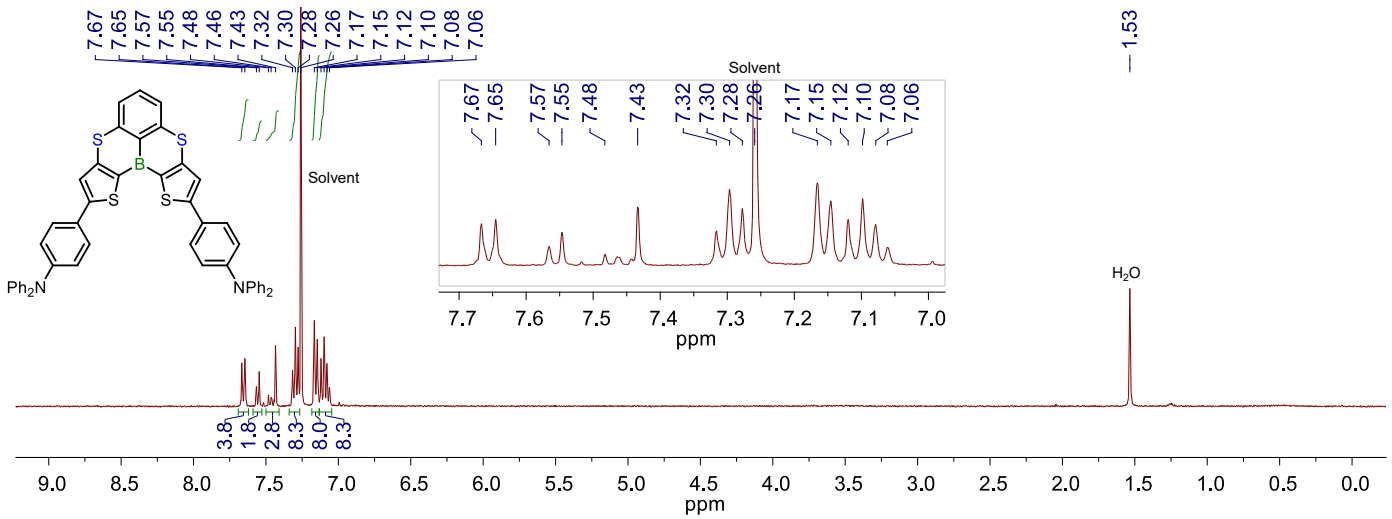

Figure S29 ^{1}H NMR spectrum of **DTTB-NPh** in $CDCl_3$ at room temperature (400 MHz).

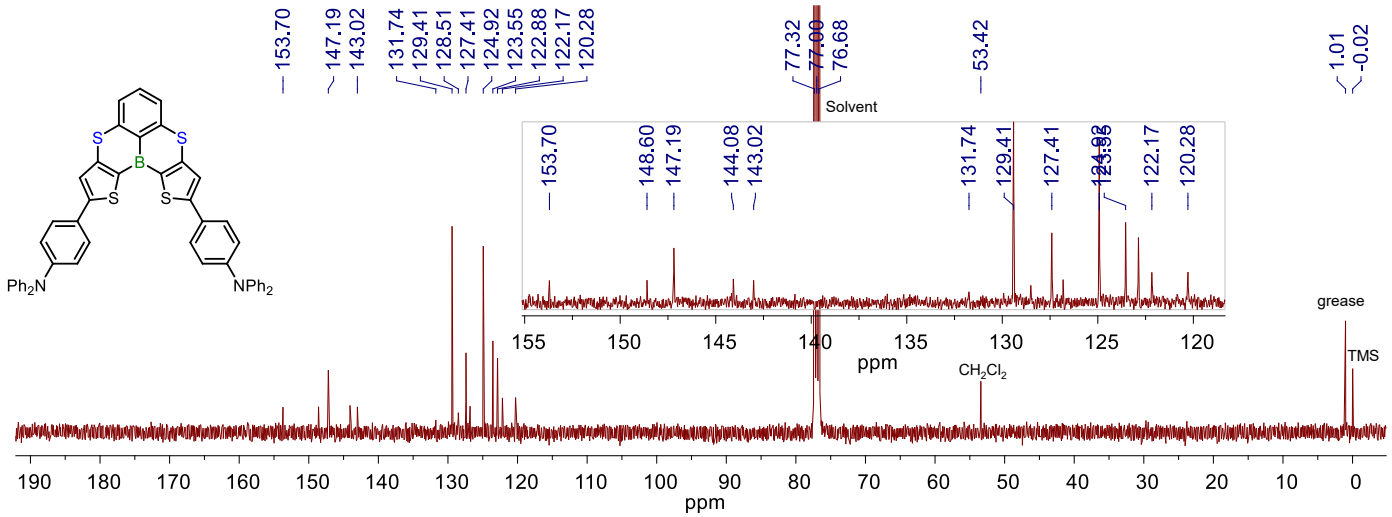

Figure S30 ^{13}C NMR spectrum of **DTTB-NPh** in $CDCl_3$ at room temperature (101 MHz).

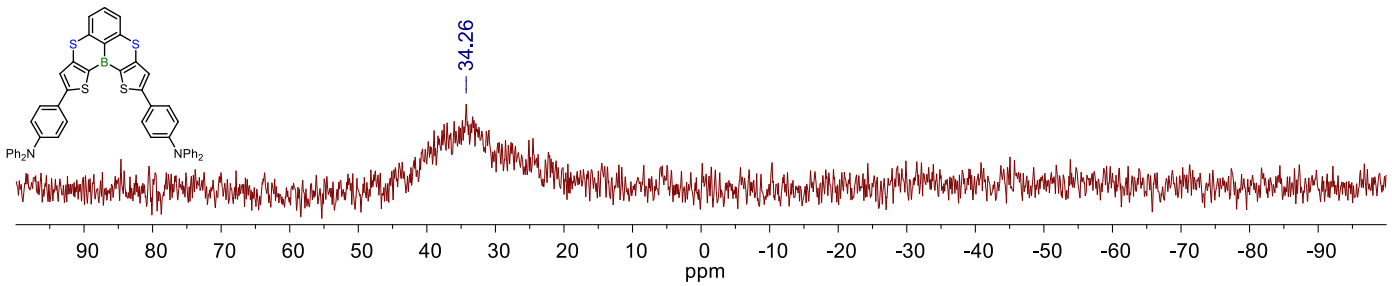

Figure S31 ^{11}B NMR spectrum of **DTTB-NPh** in $CDCl_3$ at room temperature (160 MHz).

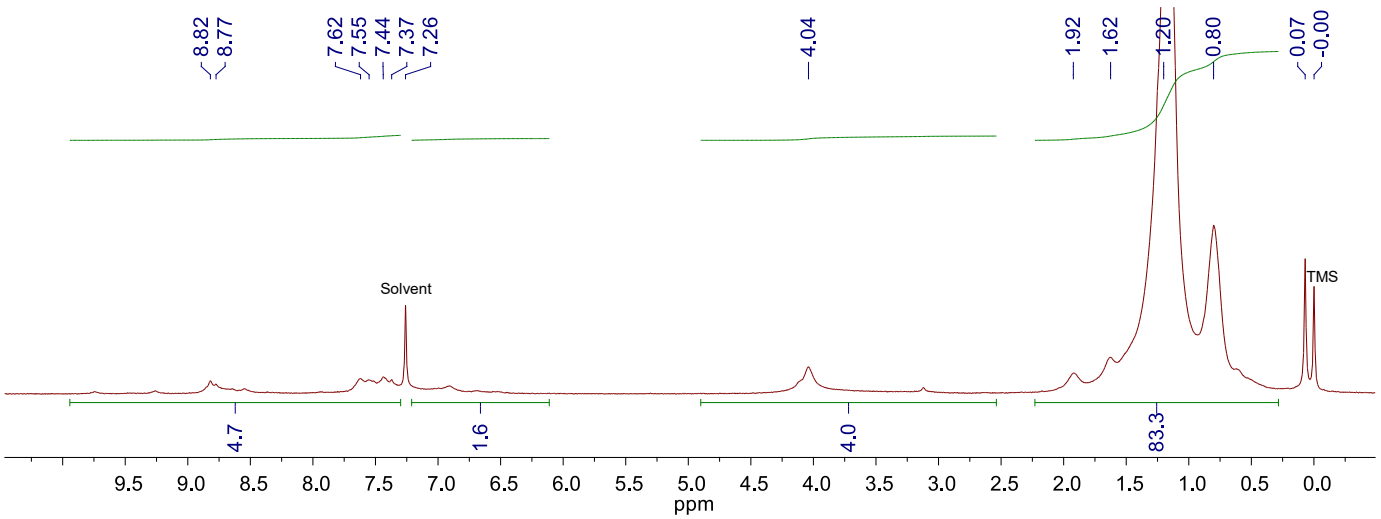

Figure S32 ^{1}H NMR spectrum of **P1** in $CDCl_3$ at room temperature (400 MHz).

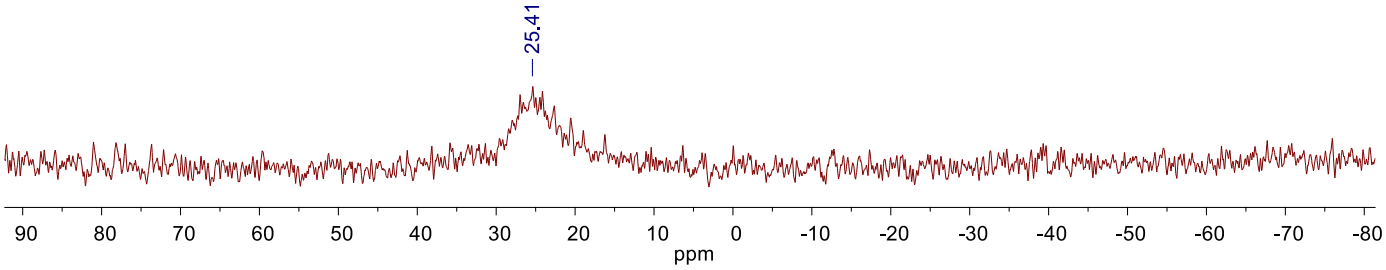

Figure S33 ^{11}B NMR spectrum of **P1** in $CDCl_3$ at 50 °C (160 MHz).

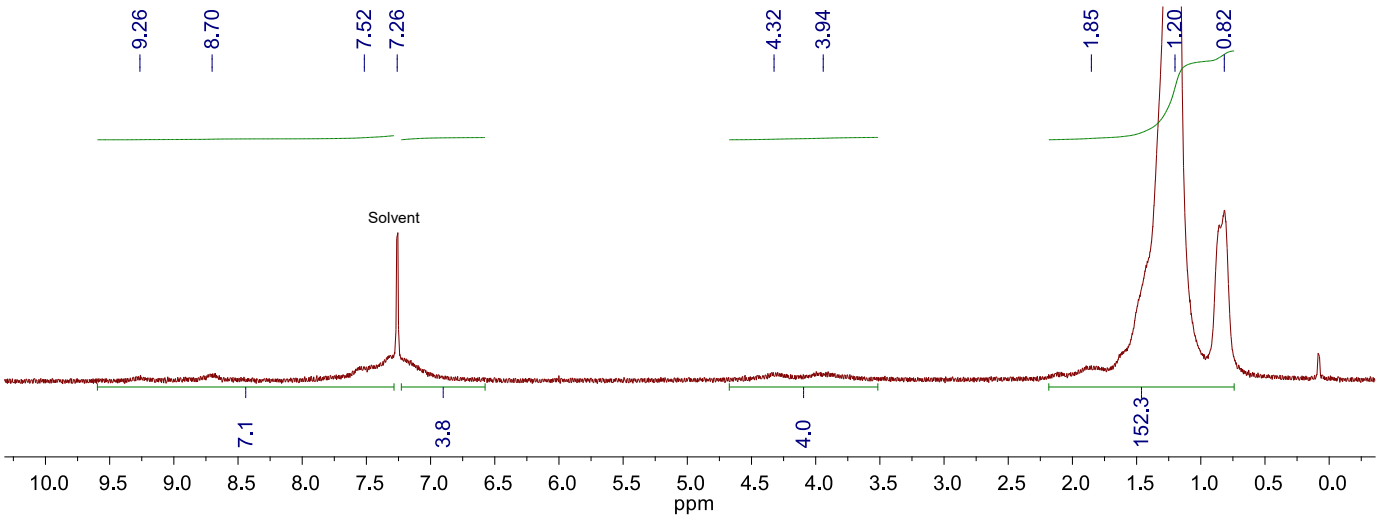

Figure S34 ^{1}H NMR spectrum of **P2** in $CDCl_3$ at 50 °C (500 MHz).

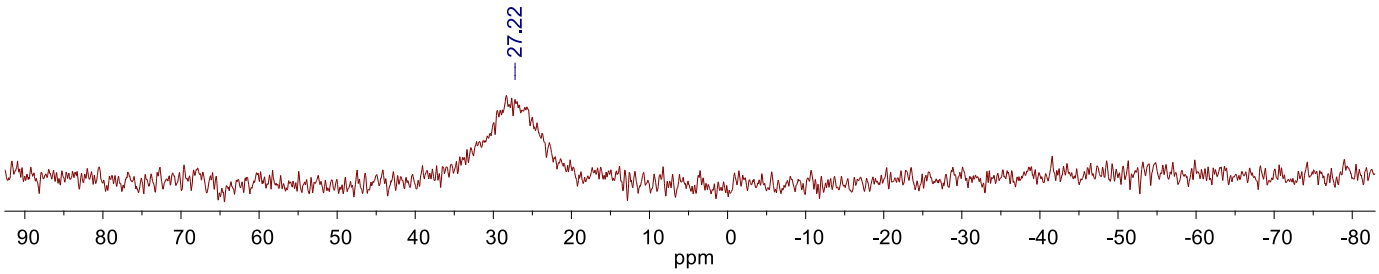

Figure S35 ^{11}B NMR spectrum of **P2** in $CDCl_3$ at 50 °C (160 MHz).

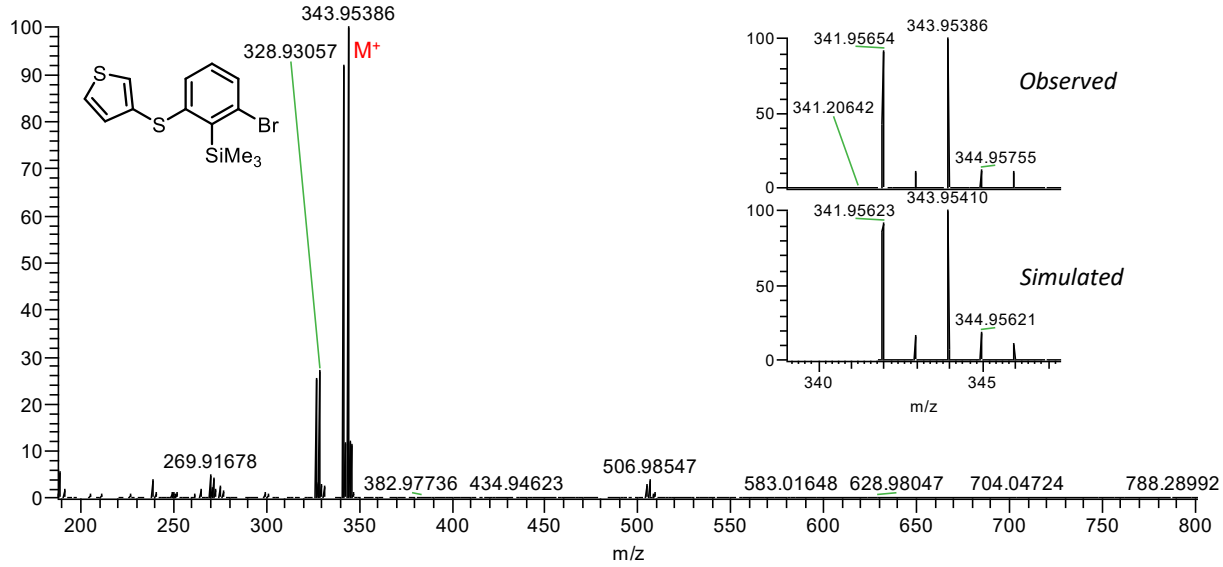

Figure S36 APCI mass spectrum of compound **2** (positive).

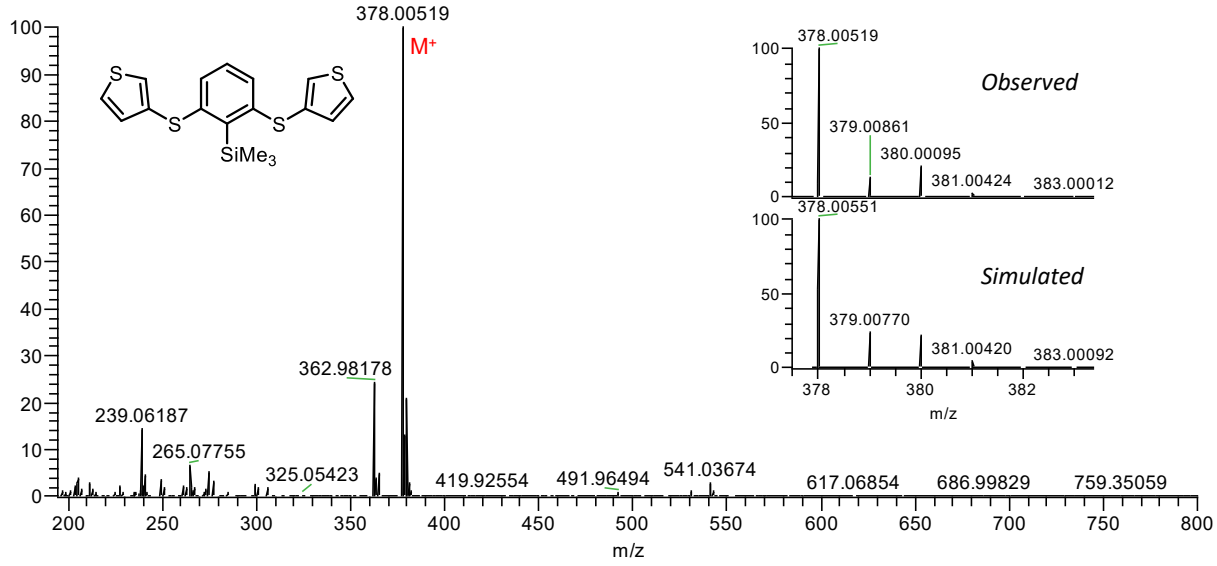

Figure S37 APCI mass spectrum of compound **3** (positive).

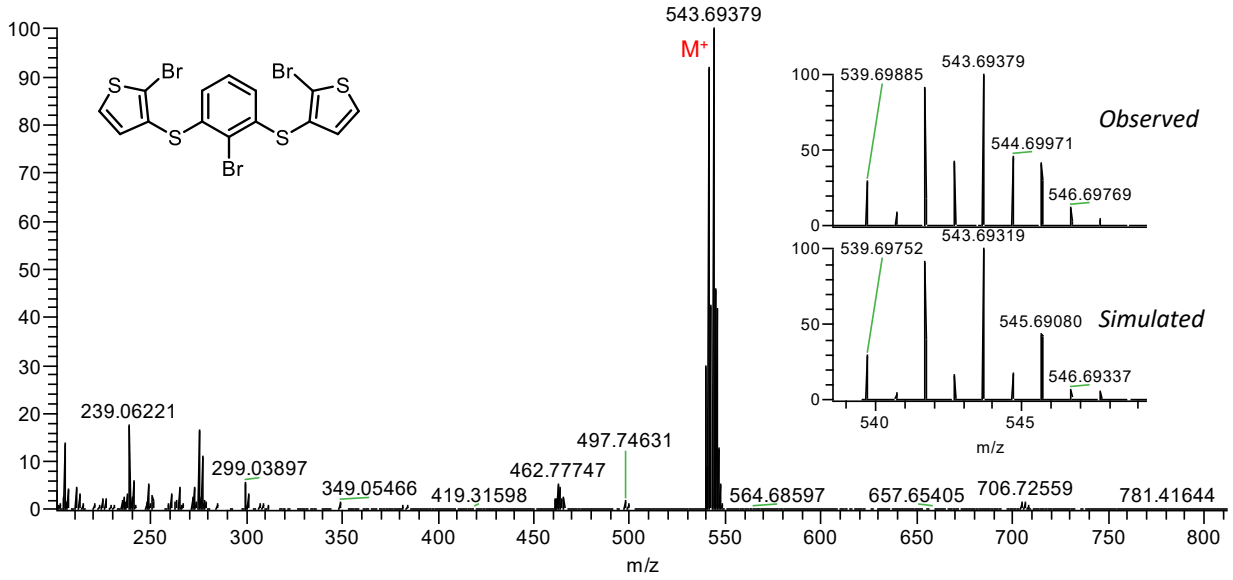

Figure S38 APCI mass spectrum of compound **4** (positive).

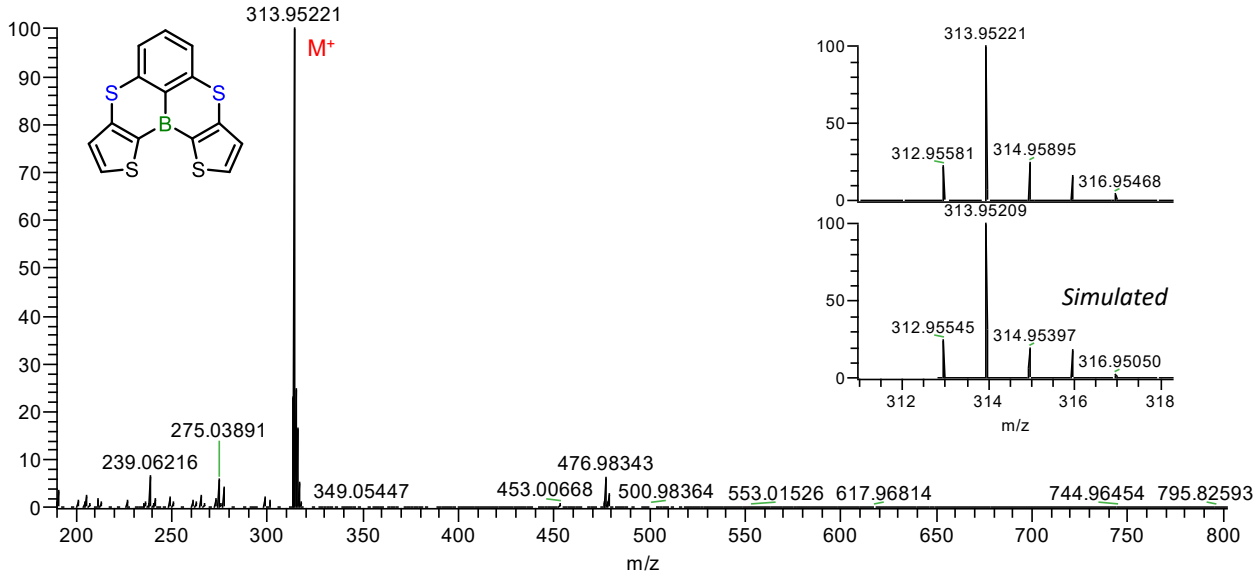

Figure S39 APCI mass spectrum of **DTTB** (positive).

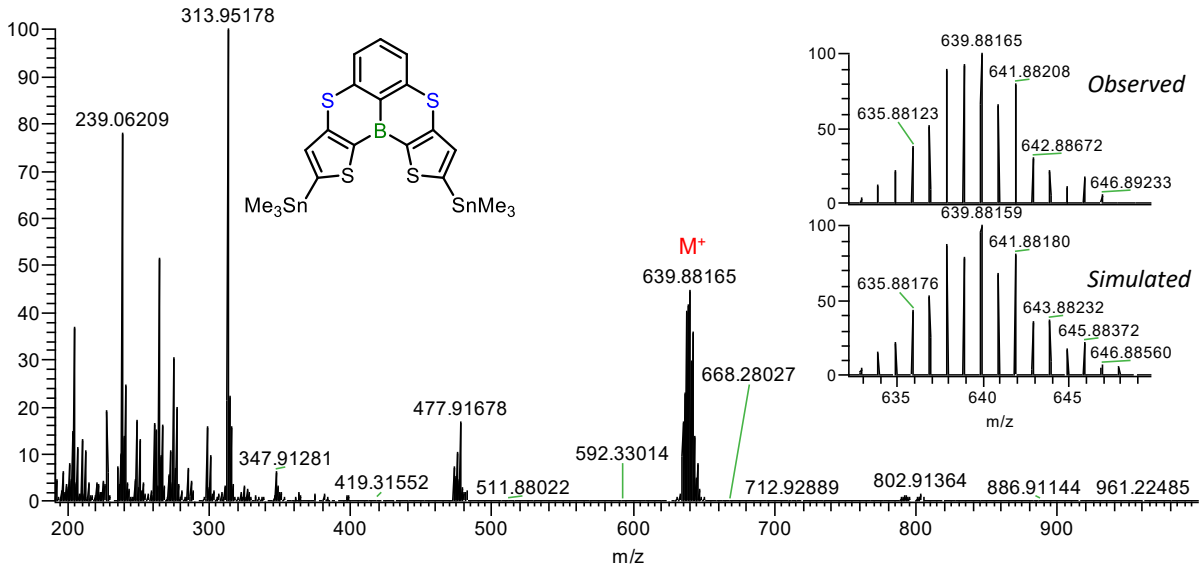

Figure S40 APCI mass spectrum of **DTTB-Sn** (positive).

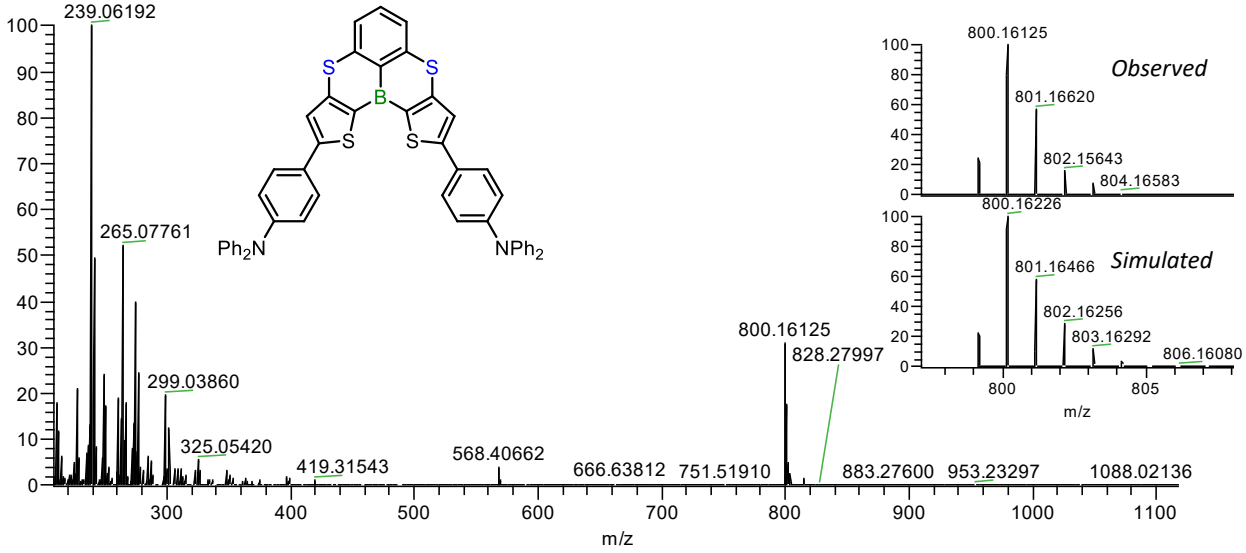

Figure S41 APCI mass spectrum of **DTTB-NPh** (positive).